Check for updates

the plant journal

SEB

The Plant Journal (2025) **122,** e70120 doi: 10.1111/tpj.70120

The cysteine protease RD19C suppresses plant immunity to *Phytophthora* by modulating copper chaperone ATX1 stability

Jingwen Dong[1], Weiwei Li[2], Yang Yang[1,2], Song Liu[1], Yilin Li[1], Yuling Meng[1] and Weixing Shan[1,*]

[1]*State Key Laboratory of Crop Stress Resistance and High-Efficiency Production and College of Agronomy, Northwest A&F University, Yangling 712100, Shaanxi, China, and*

[2]*State Key Laboratory of Crop Stress Resistance and High-Efficiency Production, and College of Plant Protection, Northwest A&F University, Yangling 712100, Shaanxi, China*

Received 16 December 2024; revised 16 February 2025; accepted 10 March 2025.
*For correspondence (e-mail wxshan@nwafu.edu.cn).

SUMMARY

Papain-like cysteine proteases (PLCPs) are pivotal in plant development and immunity, though their specific regulatory mechanisms in immune responses remain largely unexplored. In this study, we identify AtRD19C, a vacuole-localized PLCP, and demonstrate its role in negatively regulating plant immunity to *Phytophthora parasitica*. We show that AtRD19C suppresses the ethylene (ET) signaling pathway by destabilizing the copper chaperone AtATX1, which is essential for activating ET signaling through the ethylene receptor ETR1. Genetic and biochemical analyses reveal that AtATX1 and the ET signaling pathway positively regulate immunity against *Phytophthora*. Given the conserved roles of *RD19C* and *ATX1* in *Solanum tuberosum*, our findings suggest a conserved mechanism by which RD19C and ATX1 regulate resistance to *Phytophthora* across plant species.

Keywords: plant susceptibility, papain-like cysteine protease, *Phytophthora parasitica*, *RD19C*, *ATX1*, ethylene signaling pathway.

INTRODUCTION

Oomycetes are among the most destructive plant pathogens, responsible for significant crop losses and damage to forest ecosystems (Beakes et al., 2012; Kamoun et al., 2015). For instance, *Phytophthora infestans* caused the Irish Famine and remains a major threat to potato production worldwide (Haverkort et al., 2008; Savary et al., 2019). *Phytophthora parasitica* infects the leaves and roots of over a thousand plant species (Kamoun et al., 2015). While genetic breeding for disease resistance is the most effective strategy to control crop diseases, oomycetes are notorious for their genetic variability and ability to overcome host genotype-specific resistance, making chemical fungicide application a primary method of disease control. As such, strategies derived from a deeper understanding of plant susceptibility offer promising alternatives (Bi et al., 2024; Turnbull et al., 2019; Wang et al., 2015).

In our study, we employed the *P. parasitica* – *A. thaliana* compatible interaction system to screen over 10,000 independent *A. thaliana* T-DNA insertion mutants (Meng et al., 2015; Wang et al., 2011), identifying the *RD19C* gene, which encodes a papain-like cysteine protease (PLCP).

Proteolysis is essential for protein function, degradation, and the remobilization of proteins and amino acids. PLCPs are integral in regulating protein functions, either by degrading unwanted proteins or activating protein functions through specific cleavage (Pesquet, 2012). PLCPs belong to family C1A in the Merops protease database and are divided into nine plant subfamilies (Richau et al., 2012). These proteases feature two folded domains —an α-helix and a β-sheet (Turk et al., 2001) connected to form a substrate-binding groove with the catalytic triad Cys-His-Asn. Several PLCPs have been implicated in plant–pathogen interactions (Misas-Villamil et al., 2016; Shindo & Van der Hoorn, 2008). For instance, *Arabidopsis* null mutants of the PLCP *RD21* exhibit increased susceptibility to the necrotrophic fungal pathogen *Botrytis cinerea* (Shindo et al., 2012), while antisense lines lacking the tomato PLCP gene *Pip1* show increased susceptibility to *Cladosporium fulvum*, *Pseudomonas syringae*, and *P. infestans* (Ilyas et al., 2015). *XCP2* negatively regulates plant resistance to *Ralstonia solanacearum* (Zhang et al., 2014), and PLCP *RD21A* is crucial for drought-induced immunity against *P. syringae* (Liu et al., 2020). Current

© 2025 Society for Experimental Biology and John Wiley & Sons Ltd.

understanding of the RD19A-like subfamily genes has primarily focused on *RD19A*. Specifically, *RD19A* enhances the dimer activity of EDS1-PAD4, while PAD4 facilitates the maturation and nuclear accumulation of processed RD19A, thereby contributing to pathogen resistance (Zeng et al., 2023). Additionally, the receptor-like cytoplasmic kinase BSK1 is required for *RD19A*-mediated disease resistance and plays a crucial role in stabilizing the RD19A protein (Li, Shao, et al., 2024). *RD19C* and its role in plant immunity we identified has not been clearly described yet.

Copper (Cu) is an essential micronutrient and cofactor for various enzymes and electron carriers. Copper chaperones are crucial for copper transport, binding cytosolic Cu(I) and delivering it to copper-dependent proteins (Burkhead et al., 2009; Mira, Vilar, et al., 2001; Robinson & Winge, 2010). ATX1 is a copper chaperone that contains a Cu-binding MXCXXC motif, essential for maintaining copper homeostasis (Shin et al., 2012).

The ethylene signaling pathway, vital for plant immunity, is initiated when ethylene binds to its receptors (Shakeel et al., 2013; Zhao & Guo, 2011). Copper ions are essential cofactors for ethylene receptors' ethylene-binding activity (Azhar et al., 2023; Binder et al., 2010; Chen et al., 2002; Rodríguez et al., 1999). ATX1 directly or indirectly transfers copper ions to the ethylene receptor ETR1 (Hoppen et al., 2019), suggesting its crucial role in regulating the ethylene response (Li et al., 2017; Yang et al., 2022). However, the involvement of ATX1 in plant immunity remains largely unexplored.

In this study, we identify the PLCP *AtRD19C* as a negative regulator of plant resistance to *Phytophthora* through a forward genetics approach. We demonstrate that AtRD19C interacts with AtATX1, leading to the degradation of AtATX1 *in vivo* and semi-*in vitro* via protease activity. Our findings show that AtATX1 enhances plant resistance by activating the ethylene signaling pathway through ETR1. Together, these results reveal that RD19C negatively regulates plant immunity by destabilizing ATX1 and inhibiting the ethylene signaling pathway.

RESULTS

AtRD19C encodes a papain-like cysteine protease and negatively regulates *A. thaliana* immunity to *P. parasitica*

To uncover the genetic basis of plant susceptibility to oomycete pathogens, we screened a collection of *A. thaliana* T-DNA insertion mutants for enhanced disease resistance to *P. parasitica* (Li et al., 2020; Lu et al., 2020; Pan et al., 2016). This screen identified mutant 3331, which was determined to carry two T-DNA insertions: one in the promoter and the other in the first exon of *AtRD19C*, a gene encoding a predicted papain-like cysteine protease. RT-qPCR analysis revealed that *AtRD19C* expression was significantly upregulated in response to *P. parasitica* infection (Figure S1).

To confirm its role in plant immunity, we used CRISPR/Cas9 genome editing to knock out *AtRD19C* in the Col-0 background via *Agrobacterium tumefaciens*-mediated transformation. Two single-guide RNAs (sgRNAs) targeting the first exon of *AtRD19C* were employed, and DNA sequencing confirmed the generation of two independent knockout lines (*rd19c-1* and *rd19c-2*) with truncated *AtRD19C* alleles (Figure S2a). Inoculation assays showed that both *rd19c-1* and *rd19c-2* mutants exhibited enhanced resistance to *P. parasitica*, as evidenced by significantly smaller lesions and reduced pathogen biomass compared with Col-0 (Figure 1a–c).

We next generated *AtRD19C* overexpression (OE) lines in the Col-0 background. RT-qPCR analysis confirmed significantly elevated *AtRD19C* expression levels in two independent OE lines (OE48 and OE51) (Figure S2b). Infection assays revealed that both OE48 and OE51 displayed significantly increased susceptibility, as indicated by larger lesion sizes and higher *P. parasitica* biomass compared with Col-0 (Figure 1a–c).

To validate the function of *AtRD19C*, we developed two complementation lines (CM4 and CM6) by introducing *AtRD19C* under its native promoter into the *rd19c-1* background. RT-qPCR analysis confirmed restored *AtRD19C* expression in both lines (Figure S2c). Infection assays demonstrated that the complementation lines exhibited larger lesion sizes and higher pathogen biomass levels compared with *rd19c-1* (Figure 1d–f). Collectively, these findings indicate that *AtRD19C* negatively regulates plant resistance to *P. parasitica*.

RD19C has high sequence similarity with the homologous RD19A and RD19B proteins in *Arabidopsis*. We analyzed their immune function in *N. benthamiana* leaves by transient expression, followed by inoculation with *P. parasitica*. *AtRD19A-GFP* expression significantly decreased lesion sizes and *P. parasitica* biomass compared with the *Flag-GFP* control. Overexpression of *AtRD19B-GFP* displayed a tendency to promote infection but was not significant in both lesion sizes and pathogen biomass compared with the *Flag-GFP* control (Figure S3). These results suggest that *AtRD19A* positively regulates plant resistance to *P. parasitica* and that the negative immune role of *AtRD19C* is specific.

Vacuolar localization of AtRD19C is required for its immune function

PLCPs exhibit diverse subcellular localizations, including the apoplast (Paulus et al., 2020), vacuole (Kang et al., 2012), and chloroplast (Frank et al., 2019). To determine the subcellular localization of AtRD19C, we fused its coding sequence to green fluorescent protein (GFP) and transiently expressed the construct in *N. benthamiana* leaves.

© 2025 Society for Experimental Biology and John Wiley & Sons Ltd.,

1365313x, 2025, 1, Downloaded from https://onlinelibrary.wiley.com/doi/10.1111/tpj.70120 by Northwest Agri & Forestry, Wiley Online Library on [05/05/2025]. See the Terms and Conditions (https://onlinelibrary.wiley.com/terms-and-conditions) on Wiley Online Library for rules of use; OA articles are governed by the applicable Creative Commons License

AtRD19C-GFP exhibited membrane-like signals near the cell wall (Figure 1h), suggesting possible apoplastic or vacuolar localization. However, following plasmolysis, the GFP signals were observed along the plasma membrane, stained with FM4-64 (Figure 1g), confirming its intracellular localization. Co-localization experiments with the vacuolar membrane marker γ-TIP-mCherry (Nelson et al., 2007; Liu et al., 2023) further established that AtRD19C resides in the vacuole (Figure 1h).

The vacuolar localization of AtRD19C depends on its vacuolar sorting determinant (VSD), the NPIR motif, recognized by vacuolar sorting receptors (VSRs). Mutating this motif (to generate AtRD19C^{AAAA}) results in apoplastic localization (Shen et al., 2013). Plasmolysis experiments showed that AtRD19C^{AAAA}-GFP fluorescence signals were observed in the apoplast and did not overlap with γ-TIP-mCherry, confirming its altered localization (Figure 2a; Figure S4).

To test whether vacuolar localization is essential for AtRD19C's immune function, we transiently expressed *AtRD19C^{AAAA}-GFP*, *AtRD19C-GFP*, and *Flag-GFP* in *N. benthamiana* leaves and inoculated them with *P. parasitica*. While *AtRD19C-GFP* expression significantly increased lesion sizes compared with *Flag-GFP*, AtRD19C^{AAAA}-GFP failed to promote *P. parasitica* colonization (Figure 2b–c; Figure S5). These results demonstrate that vacuolar localization is crucial for AtRD19C's role in promoting susceptibility to *P. parasitica*.

The cysteine protease activity of AtRD19C is vital for its immune function

Since vacuolar localization is required for AtRD19C function, and the vacuole is critical for activating mature cysteine proteases (Cheng et al., 2020), we hypothesized that AtRD19C's protease activity underpins its immune function.

To test this, we generated an inactive mutant (*AtRD19C^{EM}*) by replacing four key catalytic residues (Glutamine 158, Cysteine 164, Histidine 307, and Asparagine 334) (Misas-Villamil et al., 2016; Rawlings et al., 2009; Rawlings & Barrett, 1993; Shindo & Van der Hoorn, 2008) with alanines (Figure S6). RT-qPCR confirmed the expression of *AtRD19C^{EM}* in two independent OE lines (OE25 and OE26) (Figure S7). The activity of AtRD19C^{EM} was monitored through activity-based protein profiling (ABPP) using DCG-04, with the DCG-04-labeled proteases detected via streptavidin-HRP. In comparison to AtRD19COE48, extracts from AtRD19C^{EM}OE26 plants exhibited reduced streptavidin cross-reactivity. Similar results were also observed in *N. benthamiana*, thereby confirming their altered protease activity (Figure S8). Infection assays revealed that OE25 and OE26 lines did not enhance susceptibility, with lesion sizes and pathogen biomass comparable to Col-0 (Figure 2d–f). These results highlight the importance of protease activity for AtRD19C's immune function.

To further confirm the role of its protease activity, we applied the cysteine protease inhibitor E64, which irreversibly binds to protease active sites (D'Silva et al., 1998), to *AtRD19C*-OE48 leaves before *P. parasitica* infection. E64 treatment significantly reduced the susceptibility of OE48 plants (Figure 2g–i), reinforcing the importance of AtRD19C's protease activity.

Taken together, these findings demonstrate that AtRD19C's protease activity is indispensable for its role in enhancing susceptibility to *P. parasitica*.

AtRD19C interacts with and destabilizes AtATX1

To elucidate the regulatory mechanisms of AtRD19C-mediated plant susceptibility, we performed immunoprecipitation (IP) and liquid chromatography–tandem mass spectrometry (LC–MS/MS) to identify its target proteins. Among approximately 20 candidate proteins identified (Table S2), we focused on the copper chaperone AtATX1. The interaction between AtRD19C and AtATX1 was confirmed using split-luciferase complementation assays in *N. benthamiana* leaves. AtATX1 was fused to cLuc (the C-terminal half of firefly luciferase [Luc]) and AtRD19C to nLuc (the N-terminal half of Luc). Luciferase reconstitution was observed only in regions co-expressing *cLuc-AtATX1* and *AtRD19C-nLuc*, confirming their interaction (Figure 3a).

Further validation was provided by co-immunoprecipitation (Co-IP) assays in *N. benthamiana*. AtATX1 was fused to mCherry at its C-terminus, and the construct was transiently co-expressed with *AtRD19C-GFP*, using *Flag-GFP* as a control. AtATX1-mCherry co-immunoprecipitated with AtRD19C-GFP, whereas no interaction was detected with Flag-GFP (Figure 3b). Additionally, a pull-down assay confirmed their direct interaction *in vitro* (Figure 3c). The vacuolar fluorescence signals of AtRD19C-GFP overlapped with AtATX1-mCherry, indicating their co-localization within the vacuole (Figure S9). Collectively, these results establish that AtRD19C interacts with AtATX1 in the vacuole.

Given that AtRD19C functions as a protease in the vacuole, we hypothesized that AtATX1 may be its substrate and undergo vacuole-dependent degradation. To test this, we treated *AtATX1-mCherry*-overexpressing *A. thaliana* seedlings with Concanamycin A (ConA), an inhibitor of vacuole-dependent degradation (Dröse & Altendorf, 1997). Upon ConA treatment, AtATX1-mCherry accumulated in vacuolar punctate structures, suggesting vacuolar degradation (Figure 3d).

We next assessed whether AtRD19C mediates AtATX1 degradation by co-expressing *AtATX1-mCherry* with *AtRD19C-GFP* or *Flag-GFP* control in *N. benthamiana*. Western blot analysis revealed reduced AtATX1 abundance when co-expressed with AtRD19C, suggesting that AtRD19C destabilizes AtATX1 *in vivo* (Figure 3e–f). Mutational inactivation of AtRD19C's protease activity

© 2025 Society for Experimental Biology and John Wiley & Sons Ltd.,

1365313x, 2025, 1, Downloaded from https://onlinelibrary.wiley.com/doi/10.1111/tpj.70120 by Northwest Agri & Forestry, Wiley Online Library on [05/05/2025]. See the Terms and Conditions (https://onlinelibrary.wiley.com/terms-and-conditions) on Wiley Online Library for rules of use; OA articles are governed by the applicable Creative Commons License

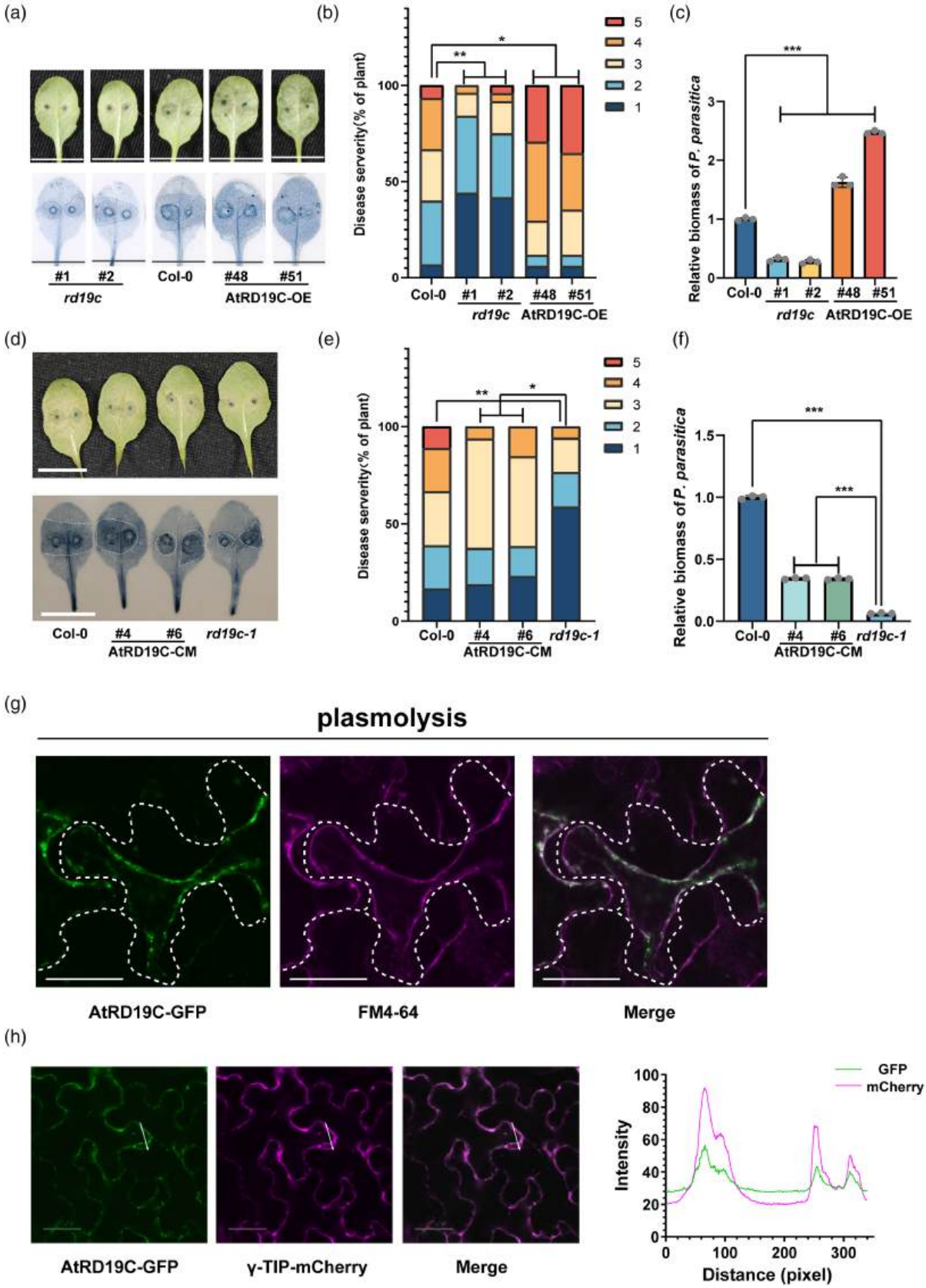

© 2025 Society for Experimental Biology and John Wiley & Sons Ltd.,

1365313x, 2025, 1, Downloaded from https://onlinelibrary.wiley.com/doi/10.1111/tpj.70120 by Northwest Agri & Forestry, Wiley Online Library on [05/05/2025]. See the Terms and Conditions (https://onlinelibrary.wiley.com/terms-and-conditions) on Wiley Online Library for rules of use; OA articles are governed by the applicable Creative Commons License

Figure 1. *AtRD19C* negatively regulates plant immunity to *P. parasitica*.
(a–c) Representative image (a), disease severity assessment (b), and *P. parasitica* biomass (c) of lesions in *rd19c* mutants, *AtRD19C*-overexpression lines (OE48 and OE51), and wild-type Col-0.
(d–f) Representative image (d), disease severity assessment (e), and *P. parasitica* biomass (f) of lesions in *rd19c-1*, *AtRD19C*-complementation lines (CM4 and CM6), and wild-type Col-0. Images were taken 72 h post-inoculation (hpi) with *P. parasitica* zoospores. Lesions were visualized using trypan blue staining. Scale bars = 1 cm. Biomass was measured by qPCR using *AtUBC9* and *PpWS041* as internal standards for *A. thaliana* and *P. parasitica*, respectively. Data represent the mean ± SD ($n = 3$). Genomic DNA was extracted from samples comprising at least five leaves at 3 days post-inoculation (dpi) per replicate. Statistical significance was assessed using Student's *t*-test for biomass analysis and Wilcoxon–Mann–Whitney test for disease severity assessment. $^{*}P < 0.05$, $^{**}P < 0.01$, and $^{***}P < 0.001$.
(g) The AtRD19C-GFP recombinant protein was transiently expressed in *N. benthamiana* leaves via agroinfiltration. Membrane dye FM4-64 was used as a membrane structure marker. Leaf epidermal peels were plasmolyzed in 2.5 M NaCl for 5 min. White dotted lines indicate the plant cell wall during plasmolysis. Scale bar = 30 μm.
(h) Subcellular localization of AtRD19C-GFP in *N. benthamiana* leaves at 3 days post-agroinfiltration (dpa) determined by confocal microscopy. γ-TIP-mCherry served as a vacuole marker. Fluorescence intensity profiles along the arrows are shown. Scale bar = 30 μm.

(AtRD19C^{EM}) abolished this destabilization, as did E64 treatment, a protease inhibitor (Figure 3e–f).

A semi-*in vitro* degradation assay further confirmed that AtRD19C directly destabilizes AtATX1. Recombinant 6 × His-AtATX1 was incubated with crude protein extracts from *AtRD19COE48*, *rd19c-1*, or Col-0 *A. thaliana* leaves. Degradation of AtATX1 was observed in *AtRD19COE48* extracts and inhibited by E64 treatment, confirming that the protease activity of AtRD19C is required for AtATX1 degradation (Figure 3g-h). Together, these results demonstrate that AtRD19C destabilizes AtATX1 through its protease activity.

AtATX1 positively regulates plant resistance to *P. Parasitica*

To explore the role of *AtATX1* in plant immunity, we obtained two T-DNA insertion mutants (*atx1-1* and *atx1-2*) and generated *AtATX1* overexpression (*AtATX1*-OE) lines in the Col-0 background using the CaMV 35S promoter. RT-qPCR analysis confirmed elevated transcript levels in two independent *AtATX1*-OE lines (OE4 and OE5) (Figure S10). Infection assays using *P. parasitica* zoospores revealed smaller lesions and reduced pathogen biomass in *AtATX1*-OE plants, whereas *atx1* mutants exhibited increased lesion sizes and pathogen loads compared with Col-0 (Figure 4a–c). These results indicate that *AtATX1* positively regulates resistance to *P. parasitica*.

To investigate the genetic relationship between *AtRD19C* and *AtATX1* in immune signaling, we generated a *rd19c-1/atx1-1* double mutant. Upon *P. parasitica* inoculation, *rd19c-1/atx1-1* plants displayed significantly higher susceptibility than *rd19c-1*, resembling wild-type Col-0 (Figure 4d–f). These results suggest that *AtATX1* functions downstream of *AtRD19C* in resistance to *P. parasitica*.

AtATX1 activates the ethylene signaling pathway

As AtATX1 facilitates ethylene (ET) signaling by delivering copper ions to the ET receptor ETR1 (Li et al., 2017; Yang et al., 2022), we tested whether this function is required for its immune role. *AtATX1OE5* plants treated with Triplin, a copper chelator, exhibited lesion sizes and pathogen biomass levels comparable to Triplin-treated controls (Figure 5a–c), suggesting that AtATX1-mediated immunity depends on copper transfer to ETR1.

To assess whether AtRD19C regulates immunity via the AtATX1-ETR1-ET pathway, we treated *rd19c-1* and Col-0 leaves with Triplin, followed by *P. parasitica* inoculation. While mock-treated *rd19c-1* plants retained enhanced resistance, triplin-treated *rd19c-1* leaves exhibited increased susceptibility, comparable to triplin-treated Col-0 plants (Figure 5d–f). These findings indicate that *rd19c-1*-mediated resistance involves ET signaling.

Using CRISPR/Cas9, we generated *etr1* knockout mutants in Col-0, *AtATX1OE5*, and *rd19c-1* backgrounds. Pathogenicity assays revealed that *etr1* mutants were more susceptible to *P. parasitica* compared with their respective parental lines, confirming the ET pathway's role in resistance (Figure 5g-i). Both *AtATX1OE5/etr1-1* and *rd19c-1/etr1-1* double mutants exhibited increased susceptibility compared with *AtATX1OE5* or *rd19c-1*, respectively (Figure 5g). Collectively, these results demonstrate that AtRD19C and AtATX1 regulate immunity via activation of the ETR1-mediated ET signaling pathway.

RT-qPCR analysis of ET pathway marker genes (*EIN3*, *EIL1*, and *ERF1*) during *P. parasitica* infection further corroborated these findings. Transcript levels of these markers were reduced in *atx1-1* and increased in *rd19c-1* compared with Col-0. Importantly, their expression in *rd19c-1/atx1-1* was lower than that in *rd19c-1*, indicating that AtRD19C activates ET signaling through AtATX1 (Figure 5j).

Our findings reveal that AtRD19C regulates the ET signaling pathway by modulating AtATX1 stability, mediating plant defense responses. This regulatory mechanism underscores the interplay between vacuolar proteases, copper chaperones, and ET signaling in plant immunity.

RD19C and ATX1 are conserved in immune functions across distant plant species

To assess the conservation of RD19C and ATX1 in immune functions across plant species, we identified homologous proteins of *AtRD19C* in *A. thaliana*, *N. benthamiana*, and *Solanum tuberosum*. Using the TAIR (https://www.

© 2025 Society for Experimental Biology and John Wiley & Sons Ltd.,

1365313x, 2025, 1, Downloaded from https://onlinelibrary.wiley.com/doi/10.1111/tpj.70120 by Northwest Agri & Forestry, Wiley Online Library on [05/05/2025]. See the Terms and Conditions (https://onlinelibrary.wiley.com/terms-and-conditions) on Wiley Online Library for rules of use; OA articles are governed by the applicable Creative Commons License

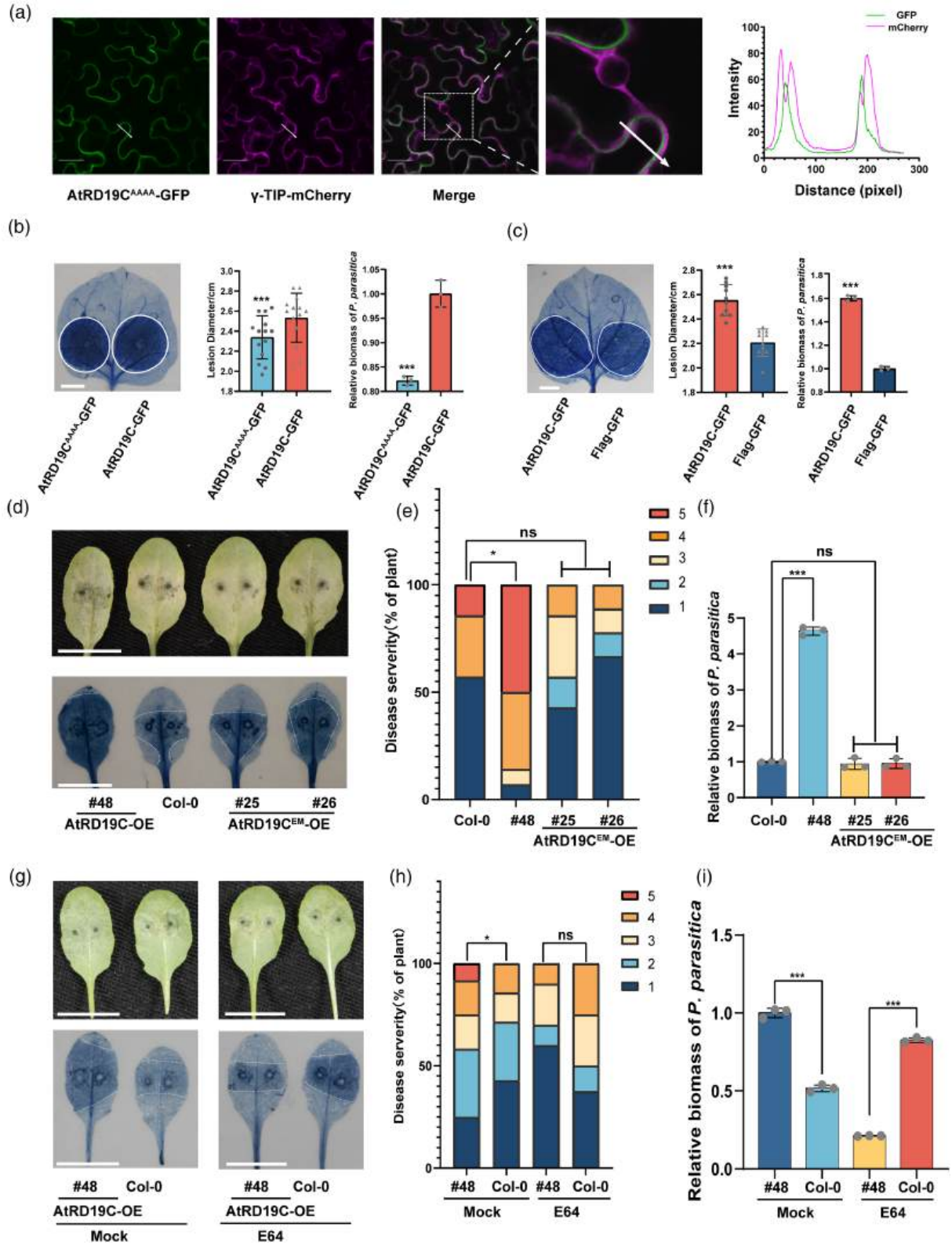

© 2025 Society for Experimental Biology and John Wiley & Sons Ltd.,

1365313x, 2025, 1, Downloaded from https://onlinelibrary.wiley.com/doi/10.1111/tpj.70120 by Northwest Agri & Forestry, Wiley Online Library on [05/05/2025]. See the Terms and Conditions (https://onlinelibrary.wiley.com/terms-and-conditions) on Wiley Online Library for rules of use; OA articles are governed by the applicable Creative Commons License

Figure 2. AtRD19C vacuolar localization and protease activity are critical for its susceptibility function.
(a) Subcellular localization of AtRD19C^{AAAA}-GFP in *N. benthamiana* leaves at three dpa analyzed by confocal microscopy. γ-TIP-mCherry served as a vacuole marker. Fluorescence intensity profiles along the arrows are shown. Scale bar = 30 μm.
(b, c) *N. benthamiana* leaves infiltrated with *A. tumefaciens* carrying *AtRD19C^{AAAA}-GFP*, *AtCRD19C-GFP*, or *Flag-GFP* were inoculated with 800 *P. parasitica* zoospores. Lesion diameters were measured at 60 hpi. *NbActin* and *PpWS041* served as internal standards for *N. benthamiana* and *P. parasitica*, respectively. Genomic DNA was extracted from samples with ten leaves at 2.5 dpi per replicate.
(d–f) Representative image (d), disease severity assessment (e), and *P. parasitica* biomass (f) of lesions in Col-0, *AtRD19C* overexpression (OE) line, and *AtRD19C^{EM}* overexpression (OE) lines at three dpi with *P. parasitica*.
(g–i) Representative images (g), disease severity assessment (h), and *P. parasitica* biomass (i) after E64 treatment. Leaves from 4-week-old *AtRD19C*-OE48 and Col-0 plants were treated with 40 μM E64 or dH_2O as a mock treatment. Scale bars = 1 cm. Statistical significance was determined using Student's *t*-test for lesion diameter and biomass analysis and Wilcoxon–Mann–Whitney test for disease severity assessment. $*P < 0.05$, $**P < 0.01$, $***P < 0.001$.

arabidopsis.org/), Sol Genomics Network (https://solgenomics.net/), and NCBI (https://www.ncbi.nlm.nih.gov/) databases, we constructed a phylogenetic tree for the cysteine protease C1A family using MEGA 7. Orthologous genes of *AtRD19C* were identified as *NbRD19C* (including *NbRD19CA* and *NbRD19CB*) in *N. benthamiana* and *StRD19C* in *S. tuberosum* (Figure S11).

To examine the immune function of *NbRD19C*, we performed virus-induced gene silencing (VIGS) in *N. benthamiana*. RT-qPCR analysis confirmed a 90% reduction in *NbRD19C* transcript levels in *TRV-NbRD19C* plants compared with *TRV-GFP* controls (Figure S12c). Silenced *NbRD19C* leaves displayed enhanced resistance to *P. parasitica* without any observable differences in growth phenotypes (Figure S12a,b,d). These findings suggest that *NbRD19C* negatively regulates immunity in *N. benthamiana*, consistent with the role of *AtRD19C* in *A. thaliana*.

In *S. tuberosum*, we generated *StRD19C*-RNAi (RNAi-1, 2, and 6) and *StRD19C*-overexpression (OE1, 2, and 6) transgenic lines in the Atlantic cultivar background. RT-qPCR analysis revealed significantly reduced (>90%) transcript levels in all RNAi lines, while the overexpression lines exhibited 4- to 10-fold higher *StRD19C* expression compared with control Atlantic plants (Figure S13a,b). No growth phenotype differences were observed between *StRD19C* transformants and GFP controls (Figure S13c). Infection assays with *P. infestans* revealed increased resistance in RNAi lines and decreased resistance in OE lines, as indicated by lesion diameters and pathogen colonization (Figure 6a–c). These results demonstrate that *StRD19C* negatively regulates immunity to *P. infestans* in *S. tuberosum*. Additionally, StRD19C localizes to the vacuole, similar to AtRD19C (Figure S14a,b), supporting conserved functionality between *A. thaliana* and *S. tuberosum*.

To investigate whether the interaction between RD19C and ATX1 is conserved in *S. tuberosum*, we identified *StATX1* as the ortholog of *AtATX1*. Co-IP experiments confirmed that StRD19C-GFP could immunoprecipitate StATX1-mCherry, indicating their interaction in *N. benthamiana* (Figure 6d). Additionally, co-expression assays revealed that StATX1-mCherry protein levels were significantly reduced when co-expressed with *StRD19C-GFP* compared with the *Flag-GFP* control (Figure 6e), demonstrating the conserved degradation of ATX1 by RD19C.

To confirm the role of *StATX1* in plant defense, we transiently expressed *StATX1-mCherry* or *Flag-GFP* (control) in *N. benthamiana* leaves, followed by infection assays. Leaves expressing *StATX1* exhibited significantly smaller lesions and reduced *P. parasitica* colonization compared with controls (Figure 6f–h), indicating that *StATX1* positively regulates immunity. Taken together, these findings demonstrate that *StRD19C* and *StATX1* perform functions similar to their orthologs in *A. thaliana*, suggesting that the immune roles of *RD19C* and *ATX1* are conserved across distant plant species.

DISCUSSION

Papain-like cysteine proteases (PLCPs) are pivotal regulators of plant immunity, characterized by their broad substrate specificity, diverse subcellular localizations, and tightly controlled activation and inactivation mechanisms (Misas-Villamil et al., 2016). Studies on PLCPs in plant immunity have primarily explored two mechanisms (Ziemann et al., 2018): (1) the generation of immune-regulating peptides from host or pathogen precursors, as seen in *Zea mays* apoplast PLCPs producing Zip1 to activate the SA signaling pathway (Ziemann et al., 2018), or vacuolar PLCPs facilitating cyclotide production (Rehm et al., 2019), and others (Chen et al., 2023; Liu, Shi, et al., 2023), (2) the targeting and proteolytic cleavage of specific immune-related substrates, such as AtXCP1, reducing RBOHD abundance to regulate PTI (Liu et al., 2023). While these roles highlight the versatility of PLCPs in immunity, their substrate selection mechanisms and broader functional landscapes remain incompletely understood.

AtRD19C is a member of the *RD19A*-like subfamily, and its role in plant immunity has not been previously reported clearly. Here, we identify AtRD19C as a vacuole-localized PLCP that participates in immunity and the ethylene (ET) signaling pathway by degrading AtATX1 (Figure 7). Our findings demonstrate that *AtRD19C* negatively regulates resistance to *P. parasitica* in *A. thaliana* (Figure 1). The vacuole, a critical organelle for developmental regulation, metabolism, and defense against biotic

© 2025 Society for Experimental Biology and John Wiley & Sons Ltd.,

1365313x, 2025, 1, Downloaded from https://onlinelibrary.wiley.com/doi/10.1111/tpj.70120 by Northwest Agri & Forestry, Wiley Online Library on [05/05/2025]. See the Terms and Conditions (https://onlinelibrary.wiley.com/terms-and-conditions) on Wiley Online Library for rules of use; OA articles are governed by the applicable Creative Commons License

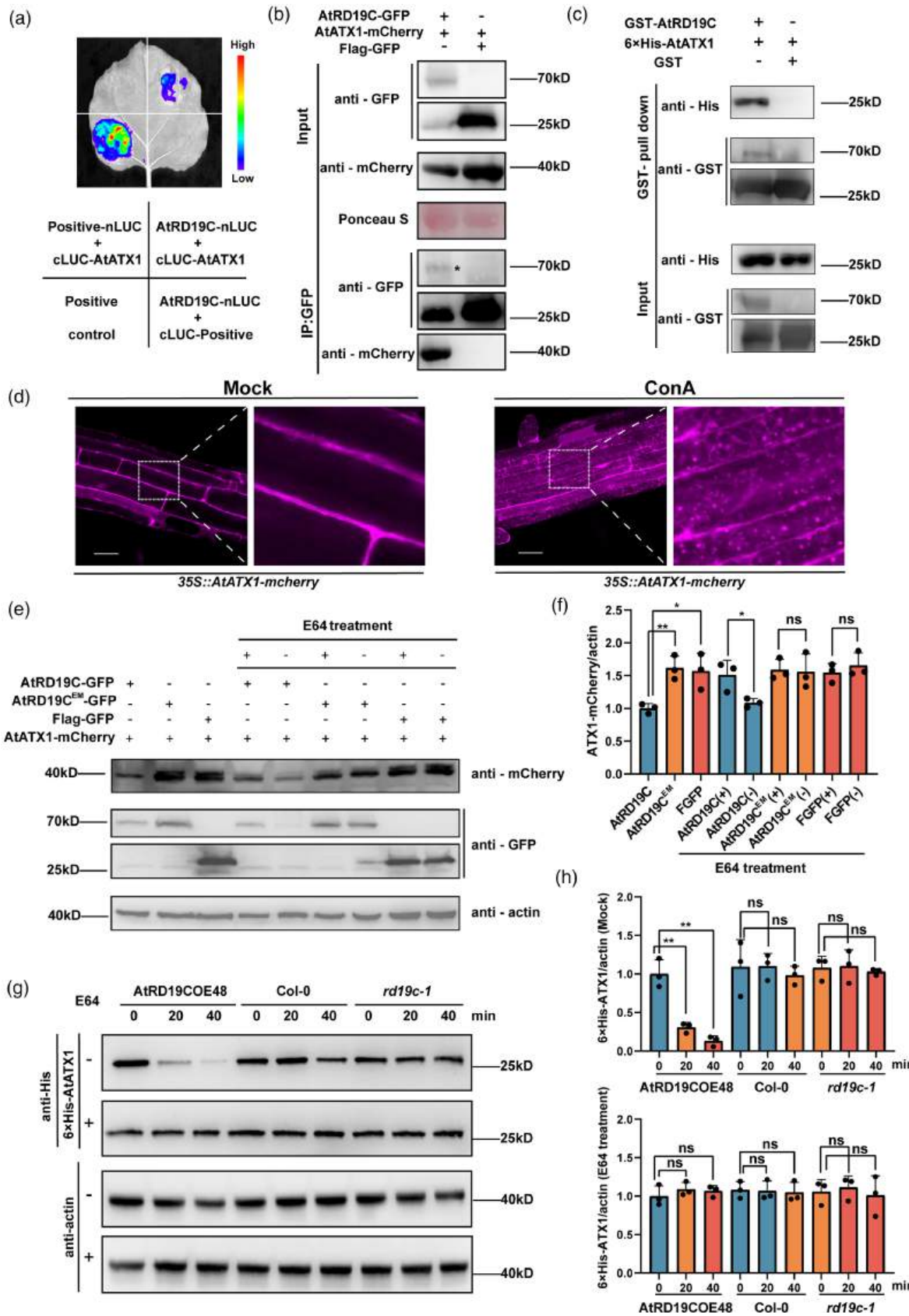

© 2025 Society for Experimental Biology and John Wiley & Sons Ltd.,

1365313x, 2025, 1, Downloaded from https://onlinelibrary.wiley.com/doi/10.1111/tpj.70120 by Northwest Agri & Forestry, Wiley Online Library on [05/05/2025]. See the Terms and Conditions (https://onlinelibrary.wiley.com/terms-and-conditions) on Wiley Online Library for rules of use; OA articles are governed by the applicable Creative Commons License

Figure 3. Interaction of AtRD19C with AtATX1.
(a) Split-luciferase assay showing interactions between AtRD19C and AtATX1. *AtRD19C-nLuc* was co-expressed with *cLuc-AtATX1* or *cLuc*-positive, and positive-*nLuc* was co-expressed with *cLuc-AtATX1*. *AtRaf36-nLuc* and *cLuc-AtMKK2* served as positive controls. Fluorescence intensity was recorded at three dpa using a CCD camera. A representative image is shown ($n = 3$).
(b) Co-immunoprecipitation assay showing AtATX1-mCherry pulled down by AtRD19C-GFP in *N. benthamiana* leaves. Total protein extracted at 72 hpi was captured with GFP-Trap beads and detected by Western blot using an anti-mCherry antibody.
(c) *In vitro* pull-down assay. 6 × His-AtATX1 and GST-AtRD19C were expressed in *E. coli* and co-incubated. Co-precipitation was detected via Western blot using anti-His and anti-GST antibodies.
(d) Concanamycin A (Con A) treatment causes AtATX1-mCherry to accumulate in vacuolar puncta. Roots of 7-day-old seedlings expressing *AtATX1-mCherry* were treated with 1 μM Con A for 24 h. Mock treatment used 1% DMSO.
(e, f) *In vivo* protein stability of AtATX1. Lane 1–3: *AtATX1-mCherry* co-expressed with *AtRD19C-GFP*, *AtRD19C^{EM}-GFP*, or *Flag-GFP* in *N. benthamiana* leaves. Lane 4–9: Infiltrated leaves treated with E64 or dH_2O at 36 hpa; protein was extracted at 60 hpa for Western blotting. Protein levels were quantified using ImageJ (mean ± SD, $n = 3$).
(g, h) Semi-*in vitro* protein stability of AtATX1. 6 × His-AtATX1 was co-incubated with crude protein extracts from *AtRD19COE48*, *rd19c-1*, or Col-0 leaves containing active PLCPs. Samples were collected at indicated time points (0, 20, 40 min) and analyzed by anti-His Western blot. PLCP activity was inhibited by E64 as a control. Protein levels were quantified using ImageJ (mean ± SD, $n = 3$).

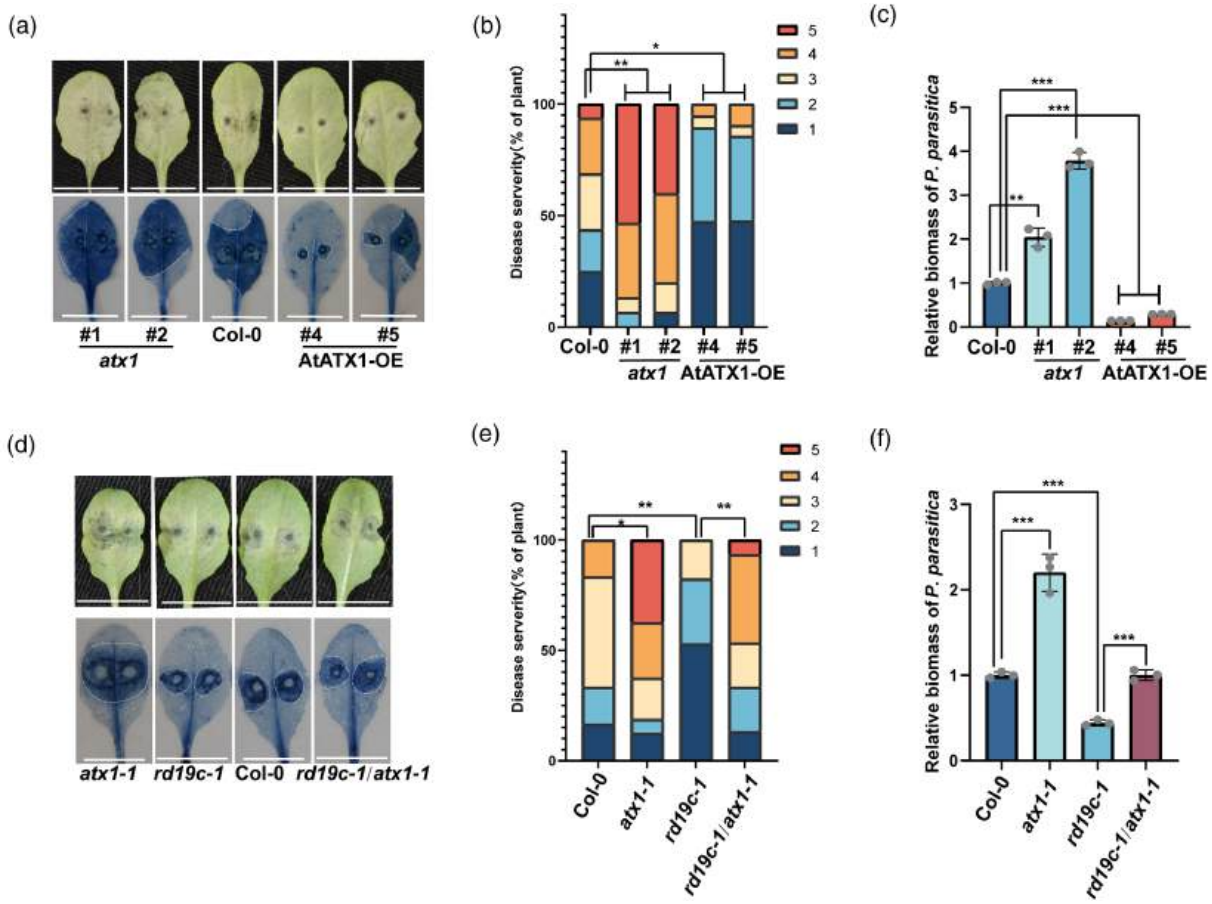

Figure 4. *AtATX1* plays an important role in plant immunity to *Phytophthora* downstream of *AtRD19C*.
(a–c) Representative image (a) and disease severity assessment (b) and *P. parasitica* biomass (c) of lesions in the *atx1* mutants, *AtATX1*-OE lines, and wild-type Col-0.
(d–f) Representative image (d) and disease severity assessment (e) and biomass (f) of *P. parasitica* lesions in wild-type Col-0, *atx1-1*, *rd19c-1*, and *rd19c-1/atx1-1*. Experiments were performed as shown in Figure 1 (a–c). $*P < 0.05$, $**P < 0.01$, $***P < 0.001$.

stresses (Hatsugai & Hara-Nishimura, 2010; Madina et al., 2019), hosts numerous hydrolases, including cysteine proteases, which facilitate the breakdown of cellular components and specific proteins (Tan et al., 2019). We show that the vacuolar localization and protease activity of AtRD19C are essential for its immune functions (Figure 2). LC–MS/MS screening identified AtATX1 as a substrate of AtRD19C (Figure 3), with subsequent assays confirming

© 2025 Society for Experimental Biology and John Wiley & Sons Ltd.,

1365313x, 2025, 1, Downloaded from https://onlinelibrary.wiley.com/doi/10.1111/tpj.70120 by Northwest Agri & Forestry, Wiley Online Library on [05/05/2025]. See the Terms and Conditions (https://onlinelibrary.wiley.com/terms-and-conditions) on Wiley Online Library for rules of use; OA articles are governed by the applicable Creative Commons License

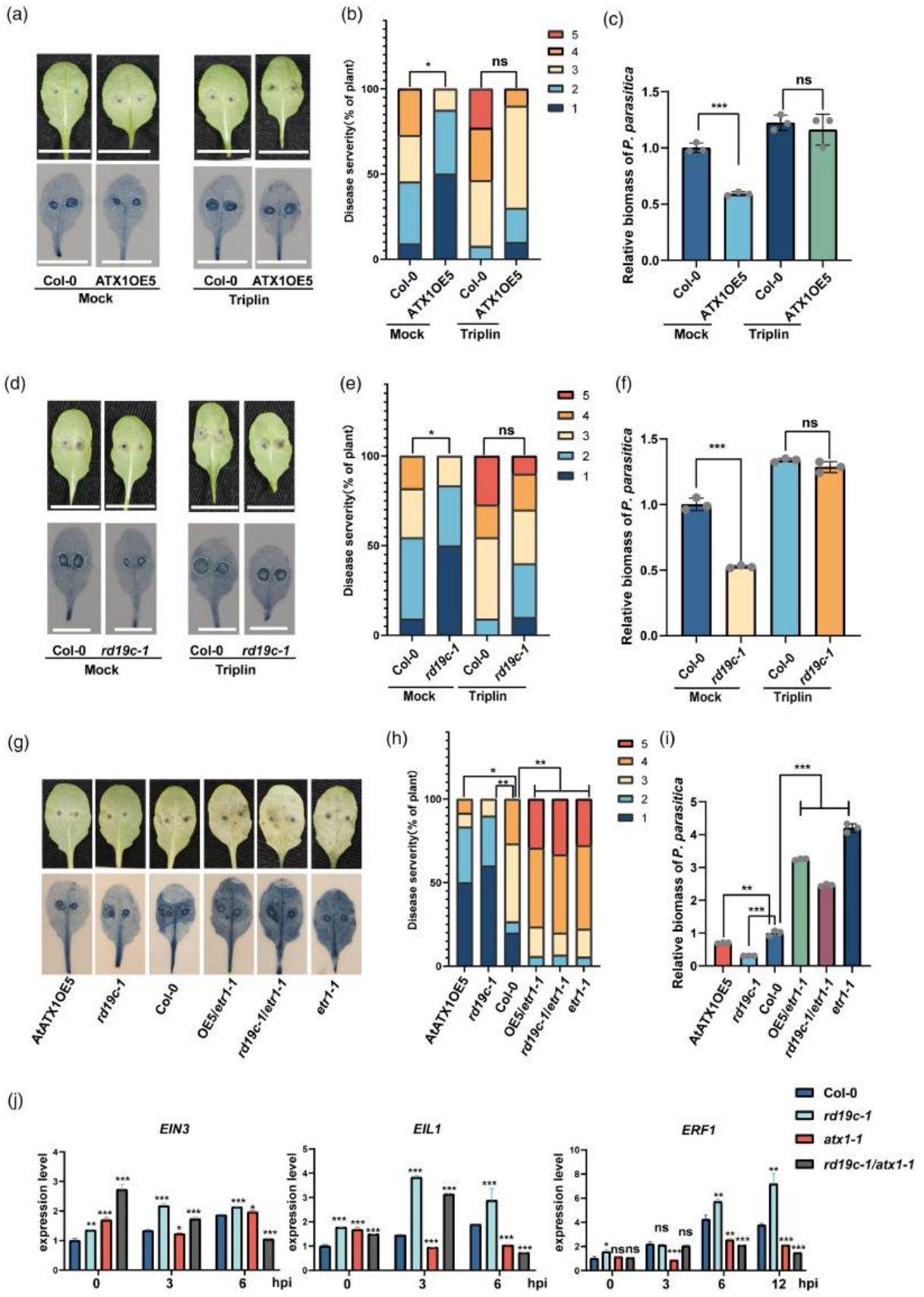

© 2025 Society for Experimental Biology and John Wiley & Sons Ltd.,

1365313x, 2025, 1, Downloaded from https://onlinelibrary.wiley.com/doi/10.1111/tpj.70120 by Northwest Agri & Forestry, Wiley Online Library on [05/05/2025]. See the Terms and Conditions (https://onlinelibrary.wiley.com/terms-and-conditions) on Wiley Online Library for rules of use; OA articles are governed by the applicable Creative Commons License

Figure 5. Activation of the ethylene pathway is required for *rd19c-1* and AtATX1 to enhance plant resistance to *P. parasitica*.
(a–c) Images (a), disease severity assessment of the infected leaves (b), and *P. parasitica* biomass (c) after treatment with Triplin. The leaves of 4-week-old AtATX1OE5 and Col-0 plants were treated with 50 μM Triplin, using 1% DMSO as a mock treatment.
(d–f) Images (d), disease severity assessment of the infected leaves (e), and *P. parasitica* biomass (f) after treatment with Triplin. The leaves of 4-week-old *rd19c-1* and Col-0 plants were treated with 50 μM Triplin.
(g–i) Images (g), disease severity assessment (h), and *P. parasitica* biomass (i) of lesions in the *AtATX1OE5*, *rd19c-1*, wild-type Col-0, *rd19c-1/etr1-1*, *AtATX1OE5/etr1-1*, and *etr1-1* lines.
(j) ET signaling pathway marker genes expression in wild-type Col-0, *atx1-1*, *rd19c-1* single mutants, and *rd19c-1/atx1-1* by RT-qPCR at different times post-inoculation. RT-qPCR data are presented as relative transcript levels for genes: We tested three marker genes, and *AtUBC9* was used as an internal control. Statistical significance was assessed by Student's *t*-test. $*P < 0.05$, $**P < 0.01$, $***P < 0.001$.

that AtRD19C degrades AtATX1 in an enzymatic activity-dependent manner (Figure 3e–h). This vacuolar mechanism underscores how AtRD19C modulates plant defense by regulating AtATX1 abundance.

AtATX1 is a copper chaperone with a conserved Cu-binding motif (Mira, Vilar, et al., 2001). It plays roles in maintaining copper homeostasis and delivering copper ions to ethylene receptors for signaling. Previous studies have shown that AtATX1 is critical for Cu tolerance under excess or deficiency (Mira, Martínez-García, & Peñarrubia, 2001) and is the primary copper donor for the ethylene receptor ETR1 (Hoppen et al., 2019; Li et al., 2017). Ethylene is a key phytohormone involved in resistance to *Phytophthora* pathogens (Li, Li, et al., 2023; Yang et al., 2019). We hypothesize that AtATX1 contributes to plant defense by activating the ET signaling pathway, a hypothesis supported by the observation that the resistance of *ATX1OE* plants to *Phytophthora* depends on the activation of ETR1 (Figure 5). Additionally, RT-qPCR results indicate that *AtRD19C* uses *AtATX1* to regulate the ET pathway, modulating plant resistance to *Phytophthora* (Figure 5).

Our study further demonstrates that *StRD19C* and *StATX1* exhibit conserved immunological roles in both *A. thaliana* and *S. tuberosum*. Notably, StRD19C degrades StATX1 in a manner analogous to its function in *Arabidopsis* (Figure 6d–e), suggesting conservation of the RD19C-ATX1 immune pathway across species. Importantly, RNAi silencing of *StRD19C* did not result in significant changes in growth phenotypes (Figure S14c), highlighting its potential application in breeding for improved late blight resistance in potato cultivation (Zhang et al., 2023).

In summary, we propose that RD19C negatively regulates plant immunity to *Phytophthora* by modulating the accumulation of the copper chaperone ATX1. This study presents a novel model in which PLCPs mediate the degradation of endogenous substrates via a vacuolar mechanism to influence hormone signaling and defense responses. Our findings provide new insights into the regulatory roles of PLCPs in plant immunity through proteolytic cleavage.

Host–pathogen interactions often involve modulation of plant immunity by altering the protein abundance (Li, Luo, et al., 2023; Zhang et al., 2014), transcript levels (Clark et al., 2018), or enzymatic activity (Bar-Ziv et al., 2015; Clark et al., 2018; Lozano-Torres et al., 2012; Pérez-López et al., 2021; Shabab et al., 2008; van der Linde et al., 2012). We hypothesize that *RD19C* is subject to similar regulatory mechanisms. Future research will aim to identify upstream regulators of *RD19C*, further elucidate the RD19C–ATX1 pathway, and uncover mechanisms underlying plant resistance to *Phytophthora*.

EXPERIMENTAL PROCEDURES

Plants and growth conditions

The wild-type, mutant, and transgenic lines of *A. thaliana* were all in the Col-0 background. The T-DNA insertion mutants, *atx1-1* (SALK_021013C) and *atx1-2* (SALK_026221C), were acquired from AraShare (https://www.arashare.cn/index/). The *rd19c-1/atx1-1* double mutant was generated by crossing the single mutants. The *rd19c-1*, *rd19c-2*, *AtATX1OE5/etr1-1*, *rd19c-1/etr1-1*, *etr1-1*, *pro35S::AtRD19C*, *proAtRD19C::AtRD19C*, *pro35S::AtRD19C^{EM}*, *pro35S::AtATX1*, and *pro35S::AtATX1-mCherry* were generated via floral dip-mediated transformation (Zhang et al., 2006) and selected on half-strength Murashige and Skoog (1/2 MS) plates with appropriate antibiotics. CRISPR/Cas9-edited mutants were identified through PCR amplification and DNA sequencing.

The silenced and overexpressed stable transgenic lines of *S. tuberosum* were developed in the Atlantic cultivar genetic background using the *Agrobacterium tumefaciens*-mediated transformation method (Sun et al., 2016). These lines were screened on Murashige and Skoog Basal Medium with Vitamins (M519) supplemented with the appropriate antibiotics.

A. thaliana, *N. benthamiana*, and *S. tuberosum* plants were grown under 11-h light/24-h dark cycles at 23°C.

Vector construction

For *pro35S::AtRD19C* and *pro35S::AtATX1*, the full-length coding sequences of *AtRD19C* and *AtATX1* were amplified from Col-0 cDNA using gene-specific primers and inserted between the *Xho*I and *Xba*I sites of the PAPK vector (Gleave, 1992; Gou et al., 2022). For *pro35S::AtRD19C-GFP* and *pro35S::AtATX1-mCherry*, the CDS of *AtRD19C* was cloned into the pART27-GFP vector at the *Xho*I site, and the CDS of *AtATX1* was inserted between the *Xho*I and *EcoR*I sites of the pART27-mCherry vector (Fan et al., 2018). For *pro35S::StRD19C*, *StRD19C* (*PGSC0003DMT400009507*) was amplified from the cDNA of the potato Atlantic cultivar and inserted between the *Xho*I and *Xba*I sites of the PAPK vector. For the *AtRD19C* complementation construct, full-length *AtRD19C* was amplified from Col-0 cDNA, and the native promoter region was amplified from Col-0 DNA and cloned into the PAPK vector with *Sca*I and *Xba*I sites.

© 2025 Society for Experimental Biology and John Wiley & Sons Ltd.,

1365313x, 2025, 1, Downloaded from https://onlinelibrary.wiley.com/doi/10.1111/tpj.70120 by Northwest Agri & Forestry, Wiley Online Library on [05/05/2025]. See the Terms and Conditions (https://onlinelibrary.wiley.com/terms-and-conditions) on Wiley Online Library for rules of use; OA articles are governed by the applicable Creative Commons License

In LCI assays, the CDS of *AtRD19C* and *AtATX1* were cloned into the pCAMBIA1300-NLuc or pCAMBIA1300-CLuc vectors using the *Kpn*I and *Sal*I sites (Zhou et al., 2018).

To generate *rd19c* mutants, two 20-bp sequences targeting *AtRD19C* (sgRNA1 and sgRNA2) were designed using CRISPR-P 2.0 (http://crispr.hzau.edu.cn/CRISPR2/) and inserted into the

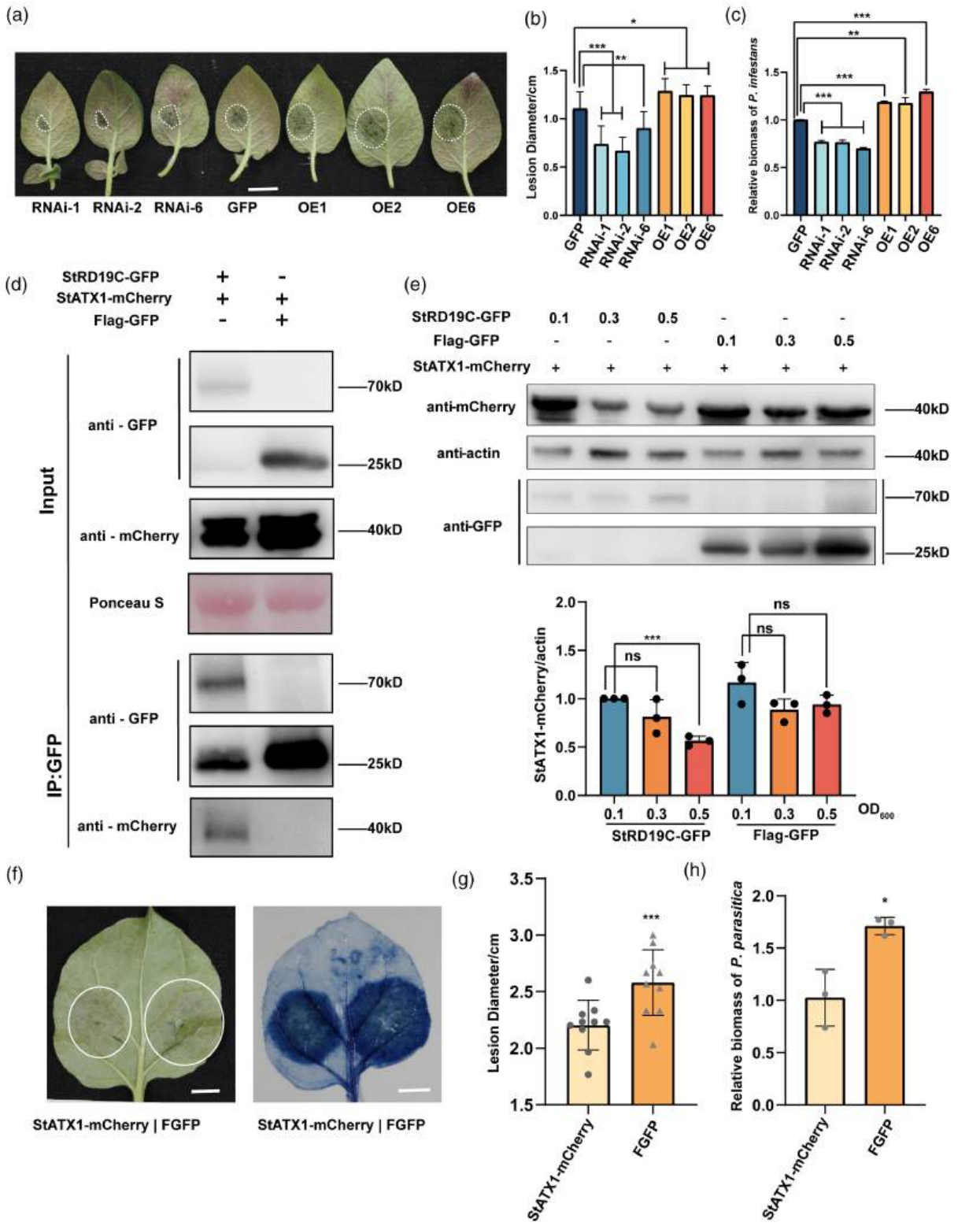

© 2025 Society for Experimental Biology and John Wiley & Sons Ltd.,

1365313x, 2025, 1, Downloaded from https://onlinelibrary.wiley.com/doi/10.1111/tpj.70120 by Northwest Agri & Forestry, Wiley Online Library on [05/05/2025]. See the Terms and Conditions (https://onlinelibrary.wiley.com/terms-and-conditions) on Wiley Online Library for rules of use; OA articles are governed by the applicable Creative Commons License

Figure 6. In distantly related plant species, the immune function of *RD19C* is conserved.
(a–c) Image (a), lesion diameters (b), and biomass (c) of *P. infestans* lesions of the *StRD19C* RNAi and overexpression (OE) transgenic lines and GFP transgenic line after inoculation with *P. infestans* zoospores. *StEF1α* and *PiActin* were used as the internal standards for *S. tuberosum* and *P. infestans*. Scale bars = 1 cm. Significance was assessed by Student's *t*-test for lesion diameter and biomass analysis.
(d) Co-immunoprecipitation of StATX1 by StRD19C. *StRD19C-GFP* was co-expressed with *StATX1-mCherry* in *N. benthamiana* leaves, and the total protein was extracted at 72 hpi. Protein complexes were pulled down using GFP-Trap beads, and the captured proteins were detected by Western blot using anti-mCherry antibody.
(e) StRD19C affects the protein abundance of StATX1 in a concentration-dependent manner. To perform transient co-expression, *Agrobacterium tumefaciens* suspensions carrying *StRD19C-GFP* or *Flag-GFP* constructs were adjusted to OD_{600} values of 0.1, 0.3, or 0.5, respectively, and mixed with that carrying *StATX1-mCherry* constructs (OD_{600} = 0.1). The StATX1-mCherry protein levels were quantified by Western blot analysis.
(f–h) The immune function of *StATX1* is conserved in *S. tuberosum*. Images (f), lesion diameters (g), and biomass of *P. parasitica* (h) in *N. benthamiana* leaves infiltrated with *Agrobacterium tumefaciens* carrying *StATX1-mCherry* and *Flag-GFP*. Experiments were performed as described in Figure 2 (b, c). $*P < 0.05$, $**P < 0.01$, $***P < 0.001$.

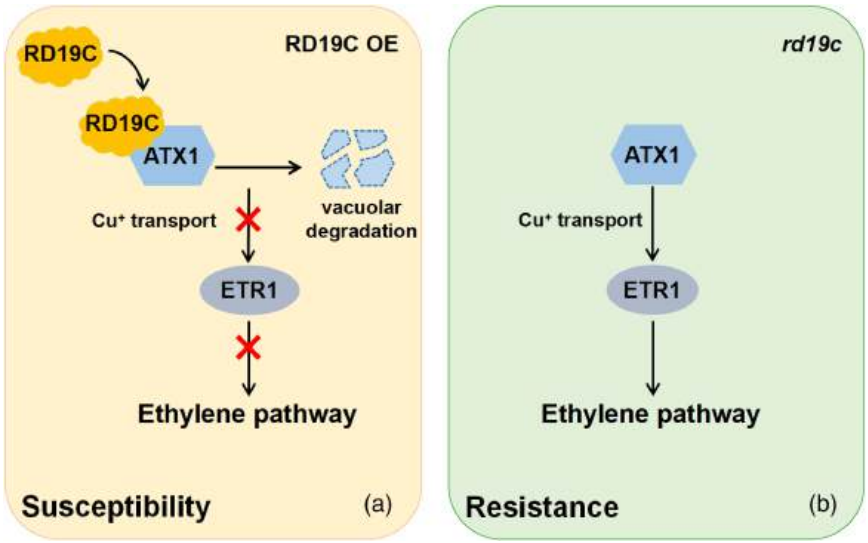

Figure 7. RD19C targets and destabilizes the ATX1 protein.
The model shows that a copper chaperone protein, ATX1, activates the ET signaling pathway through the ethylene receptor (ETR1) by copper ion transport, leading to enhanced plant resistance (b, in *rd19c* mutant plants), while the papain-like cysteine protease, RD19C, which targets and modulates the degradation of ATX1, suppresses the ET signaling pathway and interferes with plant immunity (a, in RD19C OE plants).

pKI1.1R binary vector at the *Aar*I site (Tsutsui & Higashiyama, 2017). The *etr1-1* mutant was constructed similarly.

For semi-*in vitro* assays, *AtATX1* was cloned into the pET32a vector using the *Nco*I and *Xho*I sites, while *AtRD19C* was cloned into the pGEX-6p-1 vector using *BamH*I and *Xho*I.

Primers used in this study are listed in Table S1.

VIGS in *N. Benthamiana*

The method followed Senthil-Kumar and Mysore (2014). Two sequences, designated *NbRD19CA* (*Niben101Scf01701g00013.1*) and *NbRD19CB* (*Niben101Scf06228g02005.1*), were identified. Due to high sequence similarity, both were co-silenced. *A. tumefaciens* GV3101 carrying *TRV1* and *TRV2-NbRD19C*, *TRV2-PDS*, or *TRV2-GFP* was adjusted to OD_{600} = 0.3. TRV2-PDS was used to indicate silencing. At least 10 plants were used for silencing *NbRD19C* or GFP. VIGS was performed on 3-week-old *N. benthamiana*, followed by RT-qPCR and *P. parasitica* infection assays 2 weeks post-treatment.

Inoculation assay

P. parasitica strain Pp016 and *P. infestans* strain 88069 were used. Pathogen culturing, zoospore production, and infection assays followed previous studies (Li et al., 2020; Wang et al., 2011). Infected *A. thaliana* leaves were classified into five grades based on infected area: Grade 1: hardly infected; Grade 2: lesion radius <1/4 of the leaf radius; Grade 3: lesion radius between 1/4 and 1/2 of the leaf radius; Grade 4: lesion radius >1/2–3/4 of the leaf radius; Grade 5: entire leaf infection.

RT-qPCR

Specific primers were used in 20 μL reactions with SYBR Green mix (CWBio) on a LightCycler 480 (Roche, Basel, Switzerland). Three biological replicates were included. Relative gene expression was calculated using the $2^{-\Delta\Delta Ct}$ method with housekeeping genes as references: *PpWS041* for *P. parasitica*, *AtUBC9* for *A. thaliana*, *NbActin* for *N. benthamiana*, *PiActin* for *P. infestans*, and *StEF1α* for *S. tuberosum*.

Transient expression in *N. Benthamiana*

As described in a previous study (Li et al., 2022), *A. tumefaciens* GV3101 transformed with each construct was cultured overnight in Luria-Bertani broth with antibiotics at 28°C. Cells were resuspended in infiltration buffer at OD_{600} = 0.1–0.5 and

© 2025 Society for Experimental Biology and John Wiley & Sons Ltd.,

1365313x, 2025, 1, Downloaded from https://onlinelibrary.wiley.com/doi/10.1111/tpj.70120 by Northwest Agri & Forestry, Wiley Online Library on [05/05/2025]. See the Terms and Conditions (https://onlinelibrary.wiley.com/terms-and-conditions) on Wiley Online Library for rules of use; OA articles are governed by the applicable Creative Commons License

incubated for 1–3 h at room temperature before infiltration. Assays were performed 2.5 days post-transient expression in *N. benthamiana*.

LCI assay

To perform the LCI assay, *Agrobacterium tumefaciens* GV3101 cells harboring the designated plasmids were infiltrated into *Nicotiana benthamiana* leaves for transient expression. After 2.5 days, luciferase substrate (Promega) was applied uniformly to the agroinfiltrated regions. Leaves were subjected to 5–10 min of dark treatment, and *in vivo* imaging was conducted using the PlantView100 system.

Co-IP assay

Protein extraction followed a previously described method (Li, Liu, et al., 2024). Total protein extracts were incubated with GFP Trap A beads (Chromotek) at 4°C for 4 h. For immunoblot analysis, the following antibodies were used: Mouse anti-mCherry antibody (ABclonal), Rabbit anti-GFP antibody (ABclonal), horseradish peroxidase (HRP)-conjugated goat anti-mouse IgG (L) antibody (ABclonal), and HRP-conjugated goat anti-rabbit IgG (L) antibody (ABclonal).

GST pull-down

Plasmids including pGEX-6P-1, pGEX-6P-1-*AtRD19C*, and pET32a-*AtATX1* were expressed in *E. coli* BL21. The proteins GST, GST-tagged AtRD19C, and His-tagged AtATX1 were produced under the conditions of 18°C, 120 rpm, and 1 mM isopropyl-β-D-thiogalactopyranoside (IPTG) for 16 h. The bacterial cells were pelleted, lysed, and the soluble proteins were collected. GST and GST-AtRD19C were incubated with 30 μL GST magnetic beads (Thermo Fisher Scientific) at 4°C for 2 h. After three washes, the beads were further incubated with His-tagged AtATX1 at 23°C for 1 h, followed by additional washing and boiling for 10 min. The denatured proteins were subjected to Western blot analysis.

In vivo and semi-*in vitro* protein degradation

For the *in vivo* assay, *AtRD19C-GFP*, *AtRD19C^{EM}-GFP*, or *Flag-GFP* was co-expressed in *N. benthamiana* leaves with *AtATX1-mCherry* using *A. tumefaciens*-mediated transient expression. E64 or distilled water (dH_2O) was infiltrated into leaves at 36 h post-agroinfiltration (hpa). Total protein was extracted at 60 hpa and analyzed by Western blotting.

For the semi-*in vitro* protein degradation assays were performed using soluble crude extracts were used. Recombinant 6 × His-ATX1 protein was incubated with extracts at 23°C, and samples were collected at various time points. Protein samples were precipitated with acetone and resolved in 8 M urea.

ACCESSION NUMBERS

The genes referenced in this study are associated with the following *Arabidopsis* Information Resource (https://www.arabidopsis.org/) gene accession numbers: *AtRD19C* (AT4G16190), *AtATX1* (AT1G66240), *ETR1* (AT1G66340), *EIN3* (AT3G20770), *EIL1* (AT2G27050), *ERF1* (AT3G23240); *NbRD19CA* (Niben101Scf01701g00013.1), *NbRD19CB* (Niben101Scf06228g02005.1), *StRD19C* (PGSC0003DMT400009507), and *StATX1* (PGSC0003DMT400060399) in Sol Genomics Network (https://solgenomics.net/).

AUTHOR CONTRIBUTIONS

WS and JD designed the research. JD performed most of the experiments and analyzed the data. WL, YY, SL, and YL performed the experiments. JD and WS wrote the manuscript with contributions from all authors.

ACKNOWLEDGEMENTS

This work was funded by the China Agriculture Research System (CARS-09), the National Natural Science Foundation of China (#31125022), and the Program of Introducing Talents of Innovative Discipline to Universities (project 111) from the State Administration of Foreign Experts Affairs (#B18042).

CONFLICT OF INTEREST STATEMENT

The authors declare no competing interests.

DATA AVAILABILITY STATEMENT

The data that support the findings of this study are available on request from the corresponding author. The data are not publicly available due to privacy or ethical restrictions.

SUPPORTING INFORMATION

Additional Supporting Information may be found in the online version of this article.

Figure S1. Expression pattern of *AtRD19C* during *P. parasitica* infection.

Figure S2. Expression levels of *AtRD19C* in *rd19c* mutants, CM lines, and OE lines.

Figure S3. Immune functional analysis of *AtRD19A* and *AtRD19B* by agroinfiltration-mediated transient expression in *N. benthamiana* and inoculation with *P. parasitica* zoospores.

Figure S4. Subcellular localization of AtRD19C^{AAAA}-GFP in the apoplast.

Figure S5. The protein expression of AtRD19C-GFP, AtRD19C^{AAAA}-GFP, and Flag-GFP in *P. parasitica* inoculation assays in *N. benthamiana*.

Figure S6. Schematic diagram of the AtCRD19C^{EM} mutant construct.

Figure S7. Expression levels of *AtRD19C^{EM}* in *AtRD19C^{EM}*-OE lines.

Figure S8. Abolished protease activity of AtRD19C mutant AtRD19C^{EM}.

Figure S9. Co-localization of AtRD19C and AtATX1 in the vacuole.

Figure S10. Expression levels of *AtATX1* in *atx1* mutants and *AtATX1*-OE lines.

Figure S11. Phylogenetic analysis of RD19 proteins in *A. thaliana*, *N. benthamiana*, and *S. tuberosum*.

Figure S12. Silencing of *NbRD19C* in *N. benthamiana* enhances plant resistance to *Phytophthora parasitica*.

Figure S13. Expression levels of *StRD19C* in transformant lines.

Figure S14. Subcellular localization of StRD19C-GFP in *N. benthamiana*.

Figure S15. Protein expression of AtRD19C-GFP/AtRD19C^{AAAA}-GFP/StRD19C-GFP and γ-TIP-mCherry.

Figure S16. Growth phenotypes of *rd19c* mutants, *AtRD19C*-OE lines, *AtRD19C*-complementation lines, *atx1* mutants, *AtATX1*-OE

© 2025 Society for Experimental Biology and John Wiley & Sons Ltd.,

1365313x, 2025, 1, Downloaded from https://onlinelibrary.wiley.com/doi/10.1111/tpj.70120 by Northwest Agri & Forestry, Wiley Online Library on [05/05/2025]. See the Terms and Conditions (https://onlinelibrary.wiley.com/terms-and-conditions) on Wiley Online Library for rules of use; OA articles are governed by the applicable Creative Commons License

lines, *etr1-1* mutants, *AtATX1OE5*/*etr1-1*, *rd19c-1*/*etr1-1*, and *atx1-1*/*rd19c-1* double mutants.

Table S1. Primers used in this study.

Table S2. Identification of target proteins of AtRD19C using LC-MSMS.

REFERENCES

Azhar, B.J., **Abbas, S.**, **Aman, S.**, **Yamburenko, M.V.**, **Chen, W.**, **Müller, L.** ***et al.*** (2023) Basis for high-affinity ethylene binding by the ethylene receptor ETR1 of *Arabidopsis*. *Proceedings of the National Academy of Sciences of the United States of America*, **120**, e2215195120. Available from: https://doi.org/10.1073/pnas.2215195120

Bar-Ziv, A., **Levy, Y.**, **Citovsky, V.** & **Gafni, Y.** (2015) The tomato yellow leaf curl virus (TYLCV) V2 protein inhibits enzymatic activity of the host papain-like cysteine protease CYP1. *Biochemical and Biophysical Research Communications*, **460**, 525–529. Available from: https://doi.org/10.1016/j.bbrc.2015.03.063

Beakes, G.W., **Glockling, S.L.** & **Sekimoto, S.** (2012) The evolutionary phylogeny of the oomycete "fungi". *Protoplasma*, **249**, 3–19. Available from: https://doi.org/10.1007/s00709-011-0269-2

Bi, W., **Liu, J.**, **Li, Y.**, **He, Z.**, **Chen, Y.**, **Zhao, T.** ***et al.*** (2024) CRISPR/Cas9-guided editing of a novel susceptibility gene in potato improves phytophthora resistance without growth penalty. *Plant Biotechnology Journal*, **22**, 4–6. Available from: https://doi.org/10.1111/pbi.14175

Binder, B.M., **Rodríguez, F.I.** & **Bleecker, A.B.** (2010) The copper transporter RAN1 is essential for biogenesis of ethylene receptors in *Arabidopsis*. *The Journal of Biological Chemistry*, **285**, 37263–37270. Available from: https://doi.org/10.1074/jbc.M110.170027

Burkhead, J.L., **Gogolin Reynolds, K.A.**, **Abdel-Ghany, S.E.**, **Cohu, C.M.** & **Pilon, M.** (2009) Copper homeostasis. *New Phytologist*, **182**, 799–816. Available from: https://doi.org/10.1111/j.1469-8137.2009.02846.x

Chen, Y.F., **Randlett, M.D.**, **Findell, J.L.** & **Schaller, G.E.** (2002) Localization of the ethylene receptor ETR1 to the endoplasmic reticulum of *Arabidopsis*. *The Journal of Biological Chemistry*, **277**, 19861–19866. Available from: https://doi.org/10.1074/jbc.M201286200

Chen, Y.L., **Lin, F.W.**, **Cheng, K.T.**, **Chang, C.H.**, **Hung, S.C.**, **Efferth, T.** ***et al.*** (2023) XCP1 cleaves pathogenesis-related protein 1 into CAPE9 for systemic immunity in Arabidopsis. *Nature Communications*, **14**, 4697. Available from: https://doi.org/10.1038/s41467-023-40406-7

Cheng, Z., **Guo, X.**, **Zhang, J.**, **Liu, Y.**, **Wang, B.**, **Li, H.** ***et al.*** (2020) βVPE is involved in tapetal degradation and pollen development by activating proprotease maturation in Arabidopsis thaliana. *Journal of Experimental Botany*, **71**, 1943–1955. Available from: https://doi.org/10.1093/jxb/erz560

Clark, K., **Franco, J.Y.**, **Schwizer, S.**, **Pang, Z.**, **Hawara, E.**, **Liebrand, T.W.H.** ***et al.*** (2018) An effector from the Huanglongbing-associated pathogen targets citrus proteases. *Nature Communications*, **9**, 1718. Available from: https://doi.org/10.1038/s41467-018-04140-9

Dröse, S. & **Altendorf, K.** (1997) Bafilomycins and concanamycins as inhibitors of V-ATPases and P-ATPases. *The Journal of Experimental Biology*, **200**, 1–8. Available from: https://doi.org/10.1242/jeb.200.1.1

D'Silva, I., **Poirier, G.G.** & **Heath, M.C.** (1998) Activation of cysteine proteases in cowpea plants during the hypersensitive response-a form of programmed cell death. *Experimental Cell Research*, **245**, 389–399. Available from: https://doi.org/10.1006/excr.1998.4256

Fan, G., **Yang, Y.**, **Li, T.**, **Lu, W.**, **Du, Y.**, **Qiang, X.** ***et al.*** (2018) A *phytophthora capsici* RXLR effector targets and inhibits a plant PPIase to suppress endoplasmic reticulum-mediated immunity. *Molecular Plant*, **11**, 1067–1083. Available from: https://doi.org/10.1016/j.molp.2018.05.009

Frank, S., **Hollmann, J.**, **Mulisch, M.**, **Matros, A.**, **Carrión, C.C.**, **Mock, H.P.** ***et al.*** (2019) Barley cysteine protease PAP14 plays a role in degradation of chloroplast proteins. *Journal of Experimental Botany*, **70**, 6057–6069. Available from: https://doi.org/10.1093/jxb/erz356

Gleave, A.P. (1992) A versatile binary vector system with a T-DNA organisational structure conducive to efficient integration of cloned DNA into the plant genome. *Plant Molecular Biology*, **20**, 1203–1207. Available from: https://doi.org/10.1007/bf00028910

Gou, X., **Zhong, C.**, **Zhang, P.**, **Mi, L.**, **Li, Y.**, **Lu, W.** ***et al.*** (2022) miR398b and AtC2GnT form a negative feedback loop to regulate Arabidopsis thaliana resistance against Phytophthora parasitica. *The Plant Journal*, **111**, 360–373. Available from: https://doi.org/10.1111/tpj.15792

Hatsugai, N. & **Hara-Nishimura, I.** (2010) Two vacuole-mediated defense strategies in plants. *Plant Signaling & Behavior*, **5**, 1568–1570. Available from: https://doi.org/10.4161/psb.5.12.13319

Haverkort, A.J., **Boonekamp, P.**, **Hutten, R.C.B.**, **Jacobsen, E.**, **Lotz, B.**, **Kessel, G.** ***et al.*** (2008) Societal costs of late blight in potato and prospects of durable resistance through Cisgenic modification. *Potato Research*, **51**, 47–57. Available from: https://doi.org/10.1007/s11540-008-9089-y

Hoppen, C., **Müller, L.**, **Hänsch, S.**, **Uzun, B.**, **Milić, D.**, **Meyer, A.J.** ***et al.*** (2019) Soluble and membrane-bound protein carrier mediate direct copper transport to the ethylene receptor family. *Scientific Reports*, **9**, 10715. Available from: https://doi.org/10.1038/s41598-019-47185-6

Ilyas, M., **Hörger, A.C.**, **Bozkurt, T.O.**, **van den Burg, H.A.**, **Kaschani, F.**, **Kaiser, M.** ***et al.*** (2015) Functional divergence of two secreted immune proteases of tomato. *Current Biology*, **25**, 2300–2306. Available from: https://doi.org/10.1016/j.cub.2015.07.030

Kamoun, S., **Furzer, O.**, **Jones, J.D.**, **Judelson, H.S.**, **Ali, G.S.**, **Dalio, R.J.** ***et al.*** (2015) The top 10 oomycete pathogens in molecular plant pathology. *Molecular Plant Pathology*, **16**, 413–434. Available from: https://doi.org/10.1111/mpp.12190

Kang, H., **Kim, S.Y.**, **Song, K.**, **Sohn, E.J.**, **Lee, Y.**, **Lee, D.W.** ***et al.*** (2012) Trafficking of vacuolar proteins: the crucial role of Arabidopsis vacuolar protein sorting 29 in recycling vacuolar sorting receptor. *The Plant Cell*, **24**, 5058–5073. Available from: https://doi.org/10.1105/tpc.112.103481

Li, C., **Luo, S.**, **Feng, L.**, **Wang, Q.**, **Cheng, J.**, **Xie, J.** ***et al.*** (2023) Protist ubiquitin ligase effector PbE3-2 targets cysteine protease RD21A to impede plant immunity. *Plant Physiology*, **194**, 1764–1778. Available from: https://doi.org/10.1093/plphys/kiad603

Li, J., **Deng, F.**, **Wang, H.**, **Qiang, X.**, **Meng, Y.** & **Shan, W.** (2022) The Raf-like kinase Raf36 negatively regulates plant resistance against the oomycete pathogen *Phytophthora parasitica* by targeting MKK2. *Molecular Plant Pathology*, **23**, 530–542. Available from: https://doi.org/10.1111/mpp.13176

Li, P., **Li, W.**, **Zhou, X.**, **Situ, J.**, **Xie, L.**, **Xi, P.** ***et al.*** (2023) Peronophythora litchii RXLR effector P. Litchii avirulence homolog 202 destabilizes a host ethylene biosynthesis enzyme. *Plant Physiology*, **193**, 756–774. Available from: 10.1093/plphys/kiad311

Li, Q., **Shao, J.**, **Luo, M.**, **Chen, D.**, **Tang, D.** & **Shi, H.** (2024) BRASSINOSTEROID-SIGNALING KINASE1 associates with and is required for cysteine protease RESPONSE TO DEHYDRATION 19-mediated disease resistance in *Arabidopsis*. *Plant Science*, **342**, 112033. Available from: https://doi.org/10.1016/j.plantsci.2024.112033

Li, W., **Lacey, R.F.**, **Ye, Y.**, **Lu, J.**, **Yeh, K.C.**, **Xiao, Y.** ***et al.*** (2017) Triplin, a small molecule, reveals copper ion transport in ethylene signaling from ATX1 to RAN1. *PLoS Genetics*, **13**, e1006703. Available from: https://doi.org/10.1371/journal.pgen.1006703

Li, W., **Liu, Z.**, **Huang, Y.**, **Zheng, J.**, **Yang, Y.**, **Cao, Y.** ***et al.*** (2024) *Phytophthora infestans* RXLR effector Pi23014 targets host RNA-binding protein NbRBP3a to suppress plant immunity. *Molecular Plant Pathology*, **25**, e13416. Available from: https://doi.org/10.1111/mpp.13416

Li, W., **Zhao, D.**, **Dong, J.**, **Kong, X.**, **Zhang, Q.**, **Li, T.** ***et al.*** (2020) AtRTP5 negatively regulates plant resistance to phytophthora pathogens by modulating the biosynthesis of endogenous jasmonic acid and salicylic acid. *Molecular Plant Pathology*, **21**, 95–108. Available from: https://doi.org/10.1111/mpp.12883

Liu, P., **Shi, C.**, **Liu, S.**, **Lei, J.**, **Lu, Q.**, **Hu, H.** ***et al.*** (2023) A papain-like cysteine protease-released small signal peptide confers wheat resistance to wheat yellow mosaic virus. *Nature Communications*, **14**, 7773. Available from: https://doi.org/10.1038/s41467-023-43643-y

Liu, Y., **Gong, T.**, **Kong, X.**, **Sun, J.** & **Liu, L.** (2023) XYLEM CYSTEINE PEPTIDASE 1 and its inhibitor CYSTATIN 6 regulate pattern-triggered immunity by modulating the stability of the NADPH oxidase RBOHD. *The Plant Cell*, **36**, 471–488. Available from: https://doi.org/10.1093/plcell/koad262

Liu, Y., **Wang, K.**, **Cheng, Q.**, **Kong, D.**, **Zhang, X.**, **Wang, Z.** ***et al.*** (2020) Cysteine protease RD21A regulated by E3 ligase SINAT4 is required for drought-induced resistance to pseudomonas syringae in Arabidopsis. *Journal of Experimental Botany*, **71**, 5562–5576. Available from: https://doi.org/10.1093/jxb/eraa255

Lozano-Torres, J.L., **Wilbers, R.H.**, **Gawronski, P.**, **Boshoven, J.C.**, **Finkers-Tomczak, A.**, **Cordewener, J.H.** ***et al.*** (2012) Dual disease resistance

© 2025 Society for Experimental Biology and John Wiley & Sons Ltd.,

1365313x, 2025, 1, Downloaded from https://onlinelibrary.wiley.com/doi/10.1111/tpj.70120 by Northwest Agri & Forestry, Wiley Online Library on [05/05/2025]. See the Terms and Conditions (https://onlinelibrary.wiley.com/terms-and-conditions) on Wiley Online Library for rules of use; OA articles are governed by the applicable Creative Commons License

mediated by the immune receptor Cf-2 in tomato requires a common virulence target of a fungus and a nematode. *Proceedings of the National Academy of Sciences of the United States of America*, **109**, 10119–10124. Available from: https://doi.org/10.1073/pnas.1202867109

Lu, W., **Deng, F.**, **Jia, J.**, **Chen, X.**, **Li, J.**, **Wen, Q.** ***et al.*** (2020) The Arabidopsis thaliana gene AtERF019 negatively regulates plant resistance to Phytophthora parasitica by suppressing PAMP-triggered immunity. *Molecular Plant Pathology*, **21**, 1179–1193. Available from: https://doi.org/10.1111/mpp.12971

Madina, M.H., **Rahman, M.S.**, **Zheng, H.** & **Germain, H.** (2019) Vacuolar membrane structures and their roles in plant-pathogen interactions. *Plant Molecular Biology*, **101**, 343–354. Available from: https://doi.org/10.1007/s11103-019-00921-y

Meng, Y., **Huang, Y.**, **Wang, Q.**, **Wen, Q.**, **Jia, J.**, **Zhang, Q.** ***et al.*** (2015) Phenotypic and genetic characterization of resistance in Arabidopsis thaliana to the oomycete pathogen Phytophthora parasitica. *Frontiers in Plant Science*, **6**, 378. Available from: 10.3389/fpls.2015.00378

Mira, H., **Martínez-García, F.** & **Peñarrubia, L.** (2001) Evidence for the plant-specific intercellular transport of the *Arabidopsis* copper chaperone CCH. *The Plant Journal*, **25**, 521–528. Available from: 10.1046/j.1365-313x.2001.00985.x

Mira, H., **Vilar, M.**, **Pérez-Payá, E.** & **Peñarrubia, L.** (2001) Functional and conformational properties of the exclusive C-domain from the *Arabidopsis* copper chaperone (CCH). *The Biochemical Journal*, **357**, 545–549. Available from: https://doi.org/10.1042/0264-6021:3570545

Misas-Villamil, J.C., **van der Hoorn, R.A.** & **Doehlemann, G.** (2016) Papain-like cysteine proteases as hubs in plant immunity. *New Phytologist*, **212**, 902–907. Available from: https://doi.org/10.1111/nph.14117

Nelson, B.K., **Cai, X.** & **Nebenführ, A.** (2007) A multicolored set of in vivo organelle markers for co-localization studies in *Arabidopsis* and other plants. *The Plant Journal*, **51**, 1126–1136. Available from: https://doi.org/10.1111/j.1365-313X.2007.03212.x

Pan, Q., **Cui, B.**, **Deng, F.**, **Quan, J.**, **Loake, G.J.** & **Shan, W.** (2016) RTP1 encodes a novel endoplasmic reticulum (ER)-localized protein in *Arabidopsis* and negatively regulates resistance against biotrophic pathogens. *New Phytologist*, **209**, 1641–1654. Available from: https://doi.org/10.1111/nph.13707

Paulus, J.K., **Kourelis, J.**, **Ramasubramanian, S.**, **Homma, F.**, **Godson, A.**, **Hörger, A.C.** ***et al.*** (2020) Extracellular proteolytic cascade in tomato activates immune protease Rcr3. *Proceedings of the National Academy of Sciences of the United States of America*, **117**, 17409–17417. Available from: https://doi.org/10.1073/pnas.1921101117

Pérez-López, E., **Hossain, M.M.**, **Wei, Y.**, **Todd, C.D.** & **Bonham-Smith, P.C.** (2021) A clubroot pathogen effector targets cruciferous cysteine proteases to suppress plant immunity. *Virulence*, **12**, 2327–2340. Available from: https://doi.org/10.1080/21505594.2021.1968684

Pesquet, E. (2012) Plant proteases - from detection to function. *Physiologia Plantarum*, **145**, 1–4. Available from: https://doi.org/10.1111/j.1399-3054.2012.01614.x

Rawlings, N.D. & **Barrett, A.J.** (1993) Evolutionary families of peptidases. *The Biochemical Journal*, **290**, 205–218. Available from: https://doi.org/10.1042/bj2900205

Rawlings, N.D., **Barrett, A.J.** & **Bateman, A.** (2009) MEROPS: the peptidase database. *Nucleic Acids Research*, **38**, D227–D233. Available from: https://doi.org/10.1093/nar/gkm954

Rehm, F.B.H., **Jackson, M.A.**, **De Geyter, E.**, **Yap, K.**, **Gilding, E.K.**, **Durek, T.** ***et al.*** (2019). Papain-like cysteine proteases prepare plant cyclic peptide precursors for cyclization. *Proceedings of the National Academy of Sciences*, **116**, 7831–7836. Available from:https://doi.org/10.1073/pnas.1901807116

Richau, K.H., **Kaschani, F.**, **Verdoes, M.**, **Pansuriya, T.C.**, **Niessen, S.**, **Stüber, K.** ***et al.*** (2012) Subclassification and biochemical analysis of plant papain-like cysteine proteases displays subfamily-specific characteristics. *Plant Physiology*, **158**, 1583–1599. Available from: https://doi.org/10.1104/pp.112.194001

Robinson, N.J. & **Winge, D.R.** (2010) Copper metallochaperones. *Annual Review of Biochemistry*, **79**, 537–562. Available from: https://doi.org/10.1146/annurev-biochem-030409-143539

Rodríguez, F.I., **Esch, J.J.**, **Hall, A.E.**, **Binder, B.M.**, **Schaller, G.E.** & **Bleecker, A.B.** (1999) A copper cofactor for the ethylene receptor ETR1 from *Arabidopsis*. *Science*, **283**, 996–998. Available from: https://doi.org/10.1126/science.283.5404.996

Savary, S., **Willocquet, L.**, **Pethybridge, S.J.**, **Esker, P.**, **McRoberts, N.** & **Nelson, A.** (2019) The global burden of pathogens and pests on major food crops. *Nature Ecology & Evolution*, **3**, 430–439. Available from: https://doi.org/10.1038/s41559-018-0793-y

Senthil-Kumar, M. & **Mysore, K.S.** (2014) Tobacco rattle virus-based virus-induced gene silencing in *Nicotiana benthamiana*. *Nature Protocols*, **9**, 1549–1562. Available from: https://doi.org/10.1038/nprot.2014.092

Shabab, M., **Shindo, T.**, **Gu, C.**, **Kaschani, F.**, **Pansuriya, T.**, **Chintha, R.** ***et al.*** (2008) Fungal effector protein AVR2 targets diversifying defense-related cys proteases of tomato. *The Plant Cell*, **20**, 1169–1183. Available from: https://doi.org/10.1105/tpc.107.056325

Shakeel, S.N., **Wang, X.**, **Binder, B.M.** & **Schaller, G.E.** (2013) Mechanisms of signal transduction by ethylene: overlapping and non-overlapping signalling roles in a receptor family. *AoB Plants*, **5**, plt010. Available from: https://doi.org/10.1093/aobpla/plt010

Shen, J., **Suen, P.K.**, **Wang, X.**, **Lin, Y.**, **Lo, S.W.**, **Rojo, E.** ***et al.*** (2013) An in vivo expression system for the identification of cargo proteins of vacuolar sorting receptors in Arabidopsis culture cells. *The Plant Journal*, **75**, 1003–1017. Available from: https://doi.org/10.1111/tpj.12257

Shin, L.J., **Lo, J.C.** & **Yeh, K.C.** (2012) Copper chaperone antioxidant protein1 is essential for copper homeostasis. *Plant Physiology*, **159**, 1099–1110. Available from: https://doi.org/10.1104/pp.112.195974

Shindo, T., **Misas-Villamil, J.C.**, **Hörger, A.C.**, **Song, J.** & **van der Hoorn, R.A.** (2012) A role in immunity for *Arabidopsis* cysteine protease RD21, the ortholog of the tomato immune protease C14. *PLoS One*, **7**, e29317. Available from: https://doi.org/10.1371/journal.pone.0029317

Shindo, T. & **Van der Hoorn, R.A.** (2008) Papain-like cysteine proteases: key players at molecular battlefields employed by both plants and their invaders. *Molecular Plant Pathology*, **9**, 119–125. Available from: https://doi.org/10.1111/j.1364-3703.2007.00439.x

Sun, K., **Wolters, A.M.**, **Vossen, J.H.**, **Rouwet, M.E.**, **Loonen, A.E.**, **Jacobsen, E.** ***et al.*** (2016) Silencing of six susceptibility genes results in potato late blight resistance. *Transgenic Research*, **25**(5), 731–742. Available from: https://doi.org/10.1007/s11248-016-9964-2

Tan, X., **Li, K.**, **Wang, Z.**, **Zhu, K.**, **Tan, X.** & **Cao, J.** (2019) A review of plant vacuoles: formation, located proteins, and functions. *Plants*, **8**, 327. Available from: https://doi.org/10.3390/plants8090327

Tsutsui, H. & **Higashiyama, T.** (2017) pKAMA-ITACHI vectors for highly efficient CRISPR/Cas9-mediated gene knockout in *Arabidopsis thaliana*. *Plant & Cell Physiology*, **58**, 46–56. Available from: https://doi.org/10.1093/pcp/pcw191

Turk, V., **Turk, B.** & **Turk, D.** (2001) Lysosomal cysteine proteases: facts and opportunities. *The EMBO Journal*, **20**, 4629–4633. Available from: https://doi.org/10.1093/emboj/20.17.4629

Turnbull, D., **Wang, H.**, **Breen, S.**, **Malec, M.**, **Naqvi, S.**, **Yang, L.** ***et al.*** (2019) AVR2 targets BSL family members, which act as susceptibility factors to suppress host immunity. *Plant Physiology*, **180**, 571–581. Available from: https://doi.org/10.1104/pp.18.01143

van der Linde, K., **Mueller, A.N.**, **Hemetsberger, C.**, **Kashani, F.**, **van der Hoorn, R.A.** & **Doehlemann, G.** (2012) The maize cystatin CC9 interacts with apoplastic cysteine proteases. *Plant Signaling & Behavior*, **7**, 1397–1401. Available from: https://doi.org/10.4161/psb.21902

Wang, X., **Boevink, P.**, **McLellan, H.**, **Armstrong, M.**, **Bukharova, T.**, **Qin, Z.** ***et al.*** (2015) A host KH RNA-binding protein is a susceptibility factor targeted by an RXLR effector to promote late blight disease. *Molecular Plant*, **8**, 1385–1395. Available from: https://doi.org/10.1016/j.molp.2015.04.012

Wang, Y., **Meng, Y.**, **Zhang, M.**, **Tong, X.**, **Wang, Q.**, **Sun, Y.** ***et al.*** (2011) Infection of *Arabidopsis thaliana* by *Phytophthora parasitica* and identification of variation in host specificity. *Molecular Plant Pathology*, **12**, 187–201. Available from: https://doi.org/10.1111/j.1364-3703.2010.00659.x

Yang, B., **Wang, Y.**, **Guo, B.**, **Jing, M.**, **Zhou, H.**, **Li, Y.** ***et al.*** (2019) The phytophthora sojae RXLR effector Avh238 destabilizes soybean Type2 GmACSs to suppress ethylene biosynthesis and promote infection. *New Phytologist*, **222**, 425–437. Available from: https://doi.org/10.1111/nph.15581

Yang, Y., **Hao, C.**, **Du, J.**, **Xu, L.**, **Guo, Z.**, **Li, D.** ***et al.*** (2022) The carboxy terminal transmembrane domain of SPL7 mediates interaction with RAN1 at the endoplasmic reticulum to regulate ethylene signalling in *Arabidopsis*. *New Phytologist*, **236**, 878–892. Available from: https://doi.org/10.1111/nph.18376

Zeng, Y., **Zheng, Z.**, **Hessler, G.**, **Zou, K.**, **Leng, J.**, **Bautor, J.** ***et al.*** (2023) Arabidopsis PHYTOALEXIN DEFICIENT 4 promotes the maturation and nuclear accumulation of immune-related cysteine protease RD19.

© 2025 Society for Experimental Biology and John Wiley & Sons Ltd.,

1365313x, 2025, 1, Downloaded from https://onlinelibrary.wiley.com/doi/10.1111/tpj.70120 by Northwest Agri & Forestry, Wiley Online Library on [05/05/2025]. See the Terms and Conditions (https://onlinelibrary.wiley.com/terms-and-conditions) on Wiley Online Library for rules of use; OA articles are governed by the applicable Creative Commons License

Journal of Experimental Botany, **75**, 1530–1546. Available from: https://doi.org/10.1093/jxb/erad454

Zhang, B., **Tremousaygue, D.**, **Denancé, N.**, **van Esse, H.P.**, **Hörger, A.C.**, **Dabos, P.** ***et al.*** (2014) PIRIN2 stabilizes cysteine protease XCP2 and increases susceptibility to the vascular pathogen Ralstonia solanacearum in Arabidopsis. *The Plant Journal*, **79**, 1009–1019. Available from: https://doi.org/10.1111/tpj.12602

Zhang, H., **Liu, Y.**, **Zhang, X.**, **Ji, W.** & **Kang, Z.** (2023) A necessary considering factor for breeding: growth-defense tradeoff in plants. *Stress Biology*, **3**, 6. Available from: https://doi.org/10.1007/s44154-023-00086-1

Zhang, X., **Henriques, R.**, **Lin, S.S.**, **Niu, Q.W.** & **Chua, N.H.** (2006) *Agrobacterium*-mediated transformation of *Arabidopsis thaliana* using the floral dip method. *Nature Protocols*, **1**, 641–646. Available from: https://doi.org/10.1038/nprot.2006.97

Zhao, Q. & **Guo, H.W.** (2011) Paradigms and paradox in the ethylene signaling pathway and interaction network. *Molecular Plant*, **4**, 626–634. Available from: https://doi.org/10.1093/mp/ssr042

Zhou, Z., **Bi, G.** & **Zhou, J.M.** (2018) Luciferase complementation assay for protein-protein interactions in plants. *Current Protocols in Plant Biology*, **3**, 42–50. Available from: https://doi.org/10.1002/cppb.20066

Ziemann, S., **van der Linde, K.**, **Lahrmann, U.**, **Acar, B.**, **Kaschani, F.**, **Colby, T.** ***et al.*** (2018) An apoplastic peptide activates salicylic acid signalling in maize. *Nature Plants*, **4**, 172–180. Available from: https://doi.org/10.1038/s41477-018-0116-y

© 2025 Society for Experimental Biology and John Wiley & Sons Ltd.,

1365313x, 2025, 1, Downloaded from https://onlinelibrary.wiley.com/doi/10.1111/tpj.70120 by Northwest Agri & Forestry, Wiley Online Library on [05/05/2025]. See the Terms and Conditions (https://onlinelibrary.wiley.com/terms-and-conditions) on Wiley Online Library for rules of use; OA articles are governed by the applicable Creative Commons License